

**NOVEL BROADBAND AND DUAL-MODE MICROSTRIP BANDPASS  
FILTER AND POWER DIVIDER**

**CHEN WEI YANG**

**A project report submitted in partial fulfilment of the  
requirements for the award of the degree of  
Bachelor (Hons.) of Electrical and Electronic Engineering**

**Faculty of Engineering and Science  
Universiti Tunku Abdul Rahman**

**May 2011**

**DECLARATION**

I hereby declare that this project report is based on my original work except for citations and quotations which have been duly acknowledged. I also declare that it has not been previously and concurrently submitted for any other degree or award at UTAR or other institutions.

Signature : \_\_\_\_\_

Name : CHEN WEI YANG

ID No. : 07UEB06717

Date : 15<sup>th</sup> April 2011

**APPROVAL FOR SUBMISSION**

I certify that this project report entitled “**NOVEL BROADBAND AND DUAL-MODE MICROSTRIP BANDPASS FILTER AND POWER DIVIDER**” was prepared by **CHEN WEI YANG** has met the required standard for submission in partial fulfilment of the requirements for the award of Bachelor of Electronic and Communications Engineering (Hons.) at Universiti Tunku Abdul Rahman.

Approved by,

Signature : \_\_\_\_\_

Supervisor : Dr. Lim Eng Hock

Date : 15<sup>th</sup> April 2011

The copyright of this report belongs to the author under the terms of the copyright Act 1987 as qualified by Intellectual Property Policy of University Tunku Abdul Rahman. Due acknowledgement shall always be made of the use of any material contained in, or derived from, this report.

© 2011, Chen Wei Yang. All right reserved.

Specially dedicated to  
my beloved parents and friends.

## ACKNOWLEDGEMENTS

First of all, I would like to thank everybody who had helped me in completing this project, especially my project supervisor, Dr. Lim Eng Hock for guiding me patiently throughout the development of the research.

Not forgotten to my family for providing me everything, such as encouragement, so that I am able to complete the project smoothly and easily. And thanks to my friends whose were taking the title under the same research supervisor, Dr. Lim Eng Hock. They kindly share their ideas with me and give me a hand when I was facing problem.

Last but not the least, I would like to special thank to thoughtful UTAR management for preparing a good environment for me to complete this project. Equipment, devices and materials have been prepared well. Moreover, they had prepared and set up the OPAC system so that I can get the journal needed and complete the literature survey successfully.

## **NOVEL BROADBAND AND DUAL-MODE MICROSTRIP BANDPASS FILTER AND POWER DIVIDER**

### **ABSTRACT**

Filter plays an important role in communication systems. It is an electronic device that allows signal in certain frequency ranges to go through. In other words, filter helps remove all the unwanted frequency components in a signal. Generally, there are four types of filters: lowpass filter, highpass filter, bandpass filter and bandstop filter. Two filters have been proposed in my project. The first one is a microstrip bandpass filter that is designed and fabricated on the Rogers Duroid 6006 substrate. The second design is a microstrip power divider. Power divider splits an input signal into two equal ones at the output ports. The input and output ports are connected through microstrip line, which is fabricated on a Rogers Duroid 6006 substrate. This project can be divided into three development stages: simulation, fabrication and experiment. High Frequency Structure Simulator (HFSS) has been used to simulate the filter and power divider. A microstrip bandpass filter and power divider will be fabricated based on the HFSS and the frequency responses will be measured by using Vector Network Analyzer (VNA) in laboratory. The measured results of the filter and power divider agree well with the simulated results. Several case studies have been completed on the proposed filter and power divider in order to study the relationship of different parameters on them. Discussions and future work have been proposed after the case studies. The proposed filter and power divider designs should be useful for compact transceiver modules.

## TABLE OF CONTENTS

<b>DECLARATION</b>	<b>ii</b>
<b>APPROVAL FOR SUBMISSION</b>	<b>iii</b>
<b>ACKNOWLEDGEMENTS</b>	<b>vi</b>
<b>ABSTRACT</b>	<b>vii</b>
<b>TABLE OF CONTENTS</b>	<b>viii</b>
<b>LIST OF FIGURES</b>	<b>xi</b>
<b>LIST OF SYMBOLS / ABBREVIATIONS</b>	<b>xiv</b>

### CHAPTER

<b>1</b>	<b>INTRODUCTION</b>	<b>1</b>
	1.1 Background	1
	1.2 Research Aims and Objectives	2
	1.3 Project Motivation	3
<b>2</b>	<b>LITERATURE REVIEW</b>	<b>4</b>
	2.1 About Microstrip Filter	4
	2.1.1 Microstrip Lines	5
	2.1.1.1 Substrate	7
	2.1.1.2 Effective Dielectric Constant	8
	2.1.1.3 Characteristic Impedance	10
	2.1.1.4 Wavelength/ Wave Velocity	13
	2.2 Dual-mode Microstrip Filter	14
	2.3 Cavity Resonator	14
	2.3.1 Elliptic Resonator Filter	15
	2.3.2 Square Resonator Filter	18

	2.3.3 Ridge Resonator Filter	23
<b>3</b>	<b>DUAL-MODE MICROSTRIP BANDPASS FILTER</b>	<b>28</b>
3.1	Background	28
3.2	Research Methodology	30
	3.2.1 Simulation Stage	30
	3.2.2 Fabrication Stage	34
	3.2.3 Experiment Stage	38
3.3	Proposed Filter Configurations	40
3.4	Results and Discussions	41
3.5	Case Studies	43
	3.5.1 Gap Distance	43
	3.5.2 Slot Dimension	44
	3.5.2.1 Length of Cavity	44
	3.5.2.2 Width of Cavity	45
	3.5.2.3 Height of Cavity	46
<b>4</b>	<b>DUAL-MODE MICROSTRIP POWER DIVIDER/ POWER SPLITTER</b>	<b>48</b>
4.1	Background	48
4.2	Research Methodology	49
	4.2.1 Simulation Stage	50
	4.2.2 Fabrication Stage	52
	4.2.3 Experiment Stage	53
4.3	Proposed Filter Configuration	54
4.4	Results and Discussions	54
4.5	Case Studies	56
	4.5.1 Gap Distance	56
	4.5.2 Cavity Dimension	58
	3.5.2.1 Length of Cavity	58
	3.5.2.2 Width of Cavity	59
	3.5.2.3 Height of Cavity	60

<b>5</b>	<b>CONCLUSION AND RECOMMENDATIONS</b>	61
5.1	Conclusion	61
5.2	Recommendation	62
	<b>REFERENCES</b>	65

## LIST OF FIGURES

FIGURE	TITLE	PAGE
2.1	Structure of microstrip filter	5
2.2	Microstrip line cross section	6
2.3	Effect of $W/H$ on $Z_0$ in case $W/H \leq 1$	12
2.4	Effect of $W/H$ on $Z_0$ in case $W/H \geq 1$	12
2.5	Layout of a second-order mode filter in an elliptic cavity resonator	16
2.6	Coupling mechanism for dual-mode filters in elliptic cavity resonators.	16
2.7	Response of a second-order Chebychev filter in a dual-mode elliptic cavity	17
2.8	Response a second-order filter with one transmission zero below the passband	17
2.9	Response of a second-order filter with one transmission zero above the passband	18
2.10	Square-SIW resonance cavity	19
2.11	Electric-field distribution of odd mode (E wall)	20
2.12	Electric-field distribution of even mode (H wall)	20
2.13	Schematic geometry of square SIW cavity dual-mode filter	21
2.14	Two modes resonant frequencies versus $d$ (with microstrip Feeding ports)	21
2.15	Influence of cylinder position in transmission zero and poles	22

2.16	Comparison between simulated and measured result	23
2.17	Top view of dual-mode ridge square cavity	24
2.18	Forth order dual-mode ridge cavity filter	24
2.19	Coupling scheme of forth order	25
2.20	Coupling scheme of forth order dual-mode ridge cavity filter when the resonances of the chamfered ridge are used as basic	25
2.21	Possible ridge configurations for dual-mode filters	26
2.22	Top-view of the layout of the filter.	26
2.23	Firth order pseudo-elliptic filter	27
3.1	Configuration of proposed filter	29
3.2	Photograph of the proposed filter	29
3.3	Comparison between simulated and measured result	30
3.4	Proposed filter configuration	33
3.5	Equivalent circuit transformed from the microstrip bandpass filter	34
3.6	Exposure response curve and cross section of the negative resist image after development	35
3.7	Steps to transfer IC patterns from a mask to silicon wafer	36
3.8	Example printed tracing paper	37
3.9	Connector	38
3.10	Calibration kit	39
3.11	Rohde & Schwarz ZVB8 Vector Network Analyzer (VNA)	40
3.12	Return loss or S-parameter of designed filter	41
3.13	Effect of gap distance	44

3.14	Effect of cavity length	45
3.15	Effect of cavity width	46
3.16	Effect of cavity height	47
4.1	(a) 3D, (b) top view of the power divider	49
4.2	Simulated and experimental reflection ( $S_{11}$ ), transmission ( $S_{21}$ and $S_{31}$ ) and isolation ( $S_{23}$ and $S_{32}$ ) responses of the power divider	49
4.3	Configuration of proposed power divider	51
4.4	Printed tracing paper	53
4.5	Experiment Stage	54
4.6	Comparison between simulated and measured result	55
4.7	Difference between phases	55
4.8	Effect of gap distance	57
4.9	Effect of cavity length	58
4.10	Effect of cavity width	59
4.11	Effect of cavity Height	60
5.1	Proposed configuration of one-three microstrip power divider	63
5.2	Simulated result	64

**LIST OF SYMBOLS / ABBREVIATIONS**

$\lambda$	wavelength, m
$f$	frequency, Hz
$c$	speed of light, m/s
$r$	dielectric constant
$\epsilon_{eff}$	effective dielectric constant
$h$	thickness of substrate, mm
$w$	width of striplines, mm
$Z_o$	characteristic impedance, $\Omega$
$Z_{in}$	input impedance, $\Omega$
$S_{11}$	reflection loss, dB
$S_{21}$	insertion loss, dB

## CHAPTER 1

### INTRODUCTION

#### 1.1 Background

Bandpass filter is an electronic device that allows signal in certain frequency ranges to go through. Most of the bandpass filters are commonly used by satellite mobiles and mobile communication systems. A filter removes the unnecessary information and data before sending to receivers. By including bandpass filters in a transceiver, the signal's sensitivity (signal to noise ratio) will be improved because the ranges of received frequency have been decreased and the contained noise is minimized. Nowadays, microstrip bandpass filters have replaced the traditional bandpass filters in various high frequency applications. This is because microstrip bandpass filter has many advantages such as minimal space utilization, low cost, excellent power transfer characteristics, easy to fabricate, high performance, and multi-frequency nature. Noticeably, there have been more than 600 publications on various microstrip filters in recent 10 years.

A dual-mode filter has advantages because it is able to operate in two frequency ranges. Comparing with those single-mode filters, a dual-mode filter can effectively provide two frequency passbands with a single structure. Global System for Mobile (GSM) mobile phone requires the usage of dual-mode filters. This is because a GSM mobile phone needs to receive GSM900 signal, operating at 900MHz frequency, and GSM1800 signal, operating at 1800MHz frequency, at the same time. To utilize the spectrum resources more effectively, a bandpass filter with

a wider band is more preferable. This is because more frequency components are able to get through in a single spectrum.

Not only that, filter size is another important parameter in filter design. It is no doubt that smaller filters are more preferred. This is because less material will then be needed and it is able to fit into other electronic systems more easily. A dual-mode, wideband, and small-size bandpass filter is designed in the project.

## **1.2 Research Aims and Objectives**

The main objective of this project is to propose and study a cavity-backed microstrip bandpass filter and investigate its performances. Not only that, the author would like to develop a one-to-two power divider with similar configuration. Understanding the basic knowledge is very important before designing the filter and power divider. It will enable the author to have a clearer mind when modifying the filter's configuration in the simulation stage. Without basic theory, the author will not understand the reasons behind each parametric modification. Changing it blindly will not gain any useful knowledge. A lot of related journals and articles can be found in IEEE Xplore database under the UTAR OPAC system. The author can refer to these journals and articles when designing his bandpass microstrip filter and microstrip power divider.

The first part of project is to design a microstrip bandpass filter that has dual-mode characteristic. The designed bandpass filter must be simple and easy to be made. The filter contains a cavity suspended behind it. Frequency response shows that the filter resonates at 1.42 GHz and 2.84 GHz. The second part in project aims at designing a microstrip power divider that has dual-mode characteristic. The power divider resonates at the frequencies of 2.10 and 6.20 GHz. Similar to the bandpass filter, there is a cavity suspended behind the power divider in order to design a dual-mode microstrip power divider.

The motivation of the project is to design a dual-mode microstrip bandpass filter that has good performances, which can be justified from the insertion loss, matching, and selectivity. A filter with low insertion loss, good matching, and high selectivity is usually considered as good filter. It is hoped that the results generated from this project to be publishable in the international journals. A lot of microstrip bandpass filters have been published in various IEEE journals. However, some of the filters are very complicated, bulky, and hard to build. This motivates the author to design a high-performing microstrip bandpass filter that is smaller in size and simpler to design.

Another motivation is to explore different resonator for dual-mode function. In fact, dual-mode resonator is attractive because each of the two modes can be used for a different application. As a result, the circuit size can be reduced by half.

## CHAPTER 2

### LITERATURE REVIEW

#### 2.1 About Microstrip Filter

With the rapid growth of commercial microwave technology, various microwave communication systems have been developed. Hence, microstrip filter plays an important role in many Radio Frequency (RF) or microwave applications. Emerging applications such as wireless communications continue to challenge RF or microwave filters with even more stringent requirements such as high performance, light weight, and lower cost. Microstrip filter is more suitable to perform in a high frequency environment. Its function is the same with other filters which is to select the desired frequency ranges.

The invention of Computer-Aid-Design (CAD) caused microstrip filter development increases rapidly in the 1980s. The CAD program was invented in the beginning of 1980s and therefore reduced the needs of draftsmen significantly. It brings big benefits to filter's design companies especially the small-sized ones. Its affordability and ability to run on personal computers allow engineers to do their own drafting work, eliminating the need for entire department. The designers can simulate the microstrip filter before fabricating it. Only the optimized microstrip filter will be fabricated and it increases its performance. In addition, the cost and fund spent will be decreased because the optimized filter will perform better, it decreases the failure in fabrication stage.

The configuration of microstrip filter is shown in Figure 2.1. It is built using three main materials, which are microstrip line, substrate, and ground. These three materials must co-exist in every microstrip filter, otherwise, it is unable to work and function. Many types of microstrip filter designs are available in the market. For examples, rectangular patch filter, circular patch filter, circular ring filter, and many others. Each microstrip filter design has its own characteristics and advantages. Different microstrip filters can be selected according to the designers' requirements.

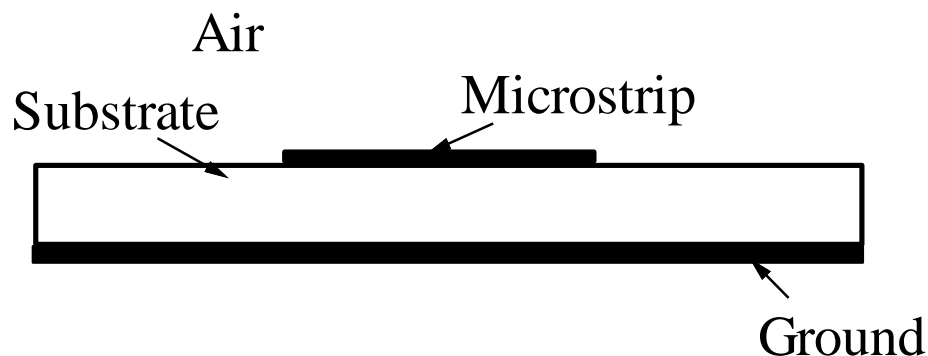


Figure 2.1: Configuration of the microstrip filter

### 2.1.1 Microstrip Lines

Microstrip line is a transmission line which is compatible with circuit construction techniques in order to provide guided waves over limited distances. It is a planar transmission line that is made on a ground plane. It employs a flat strip conductor suspended above a ground plane by a low-loss dielectric material. In other words, the microstrip transmission line is a “high grade” printed circuit construction. It consists of a track of copper or other conductor as insulating substrate. Therefore, the microstrip line can be said as a variant of a two-wire transmission line.

Microstrip line was developed by ITT laboratories as a competitor to stripline. According to Pozar, early microstrip was used as fat substrates, which allowed non-TEM waves to propagate and it led to unpredictable results. In the 1960s, the thin version of microstrip became very popular.

Figure 2.2 shows the microstrip cross section which is built on three layers of dielectrics (microstrip, substrate, and ground). It consists of a conductive microstrip with a width and a thickness of wider ground plane, separated by dielectric layer of thickness as shown below. In Figure 2.2,  $W$  stands for width,  $T$  for thickness and  $H$  for height.  $\epsilon_R$  is the relative permittivity of the substrate.

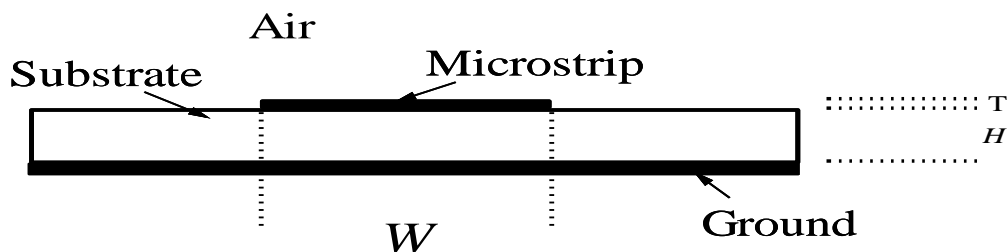


Figure 2.2: Microstrip line cross section

Besides microstrip line, stripline and coplanar waveguide can also be used to convey microwave-frequency signals. However, they are not used in this project due to some disadvantages that plague them in which could not be ignored in this project. Firstly, it is harder and more expensive to be fabricated compared with microstrip. Either lumped-element and active components have to be buried between the groundplanes, or, transitions to microstrip must be employed to get the components onto the top of the board. Secondly, the stripline widths are narrower for a given impedance and board thickness than for microstrip. So forty mils thick stripline is needed to replace ten mil thick microstrip.

On the other hand, the coplanar waveguide also has its own disadvantage. In reality, the coplanar waveguide is potentially lousy and heat dissipative. It means that surface of the coplanar waveguide could get very hot when it operates. Moreover, there is a general lack of understanding of how to employ coplanar waveguide within the microwave design community. In fact, a lot of CAD programs do not support such structure. This may be the main reason on why coplanar waveguide is not popular.

Furthermore, the microstrip also has some advantages. In fact, the major advantage of microstrip over stripline is that all active components can be mounted on top of the board. Hence, it is a convenient form of transmission line structure for

probe measurement of voltage, current, and waves. Moreover, microstrip is much cheaper than coplanar waveguide and it's lighter and more compact. However, it reported some disadvantages, particularly where the existence of two different dielectric constants (below and above the strip) makes the circuit difficult to be analyzed in closed form. Moreover, another disadvantage of microstrip will appear when high isolation is required such as in a filter or a switch because microstrip circuit can radiate, thus, causing unintended circuit response. Not only that, the microstrip has generally lower power capacity with higher losses.

The microstrip transmission line is still chosen in this project because its advantages are more obvious in filter designs. The design procedure will be easier since all of the active components are mounted on the top of the board. Moreover, the aforementioned cross-talk and unintentional radiation is not an issue in this project. A good number of professionals agree with this with their proven results published in many refereed journals.

#### **2.1.1.1 Substrate**

In the project, Rogers Duroid 6006 with permittivity of 6.15 is used as the substrate. It is a double-sided material with dimension of 25.4cm x 25.4cm. The following are the features of the Rogers Duroid 6006:

- High dielectric constant (6.15) for circuit size reduction.
- Low loss. Ideal for operating at X-band or below. Suit for high frequency application.
- Excellent electrical and mechanical properties.
- Low moisture absorption. It can reduce the effects of moisture on electrical loss.
- Tight permittivity and thickness control for repeatable circuit performance.
- Ease for fabrication and stability in use.
- Tight tolerance control.

However, there are some drawbacks for Rogers Duroid 6006. Although its properties and features are very suitable for filter designs, some of the filter designers

prefer to use FR-4 as substrate because Rogers Duroid 6006 is a type of substrates that might not common in Malaysia and has to be purchased online. It costs more time and cost for the delivery service. Next is the price problem where Rogers Duroid 6006 is considered to be expensive compared with the FR-4 substrate. So these are the reason on why designers do not choose the Rogers Duroid 6006 as substrate although they know that it will perform better. Price, good performance and easy to get in market are the advantages of FR-4 over Rogers Duroid 6006.

However, the present study selected still the Rogers Duroid 6006 as substrate because its features are very useful in the author's filters. The filter has a cavity attached behind and it brings instability problem in measuring the experiment result. Rogers Duroid 6006 helps to control the quality and reduce the error that might happen. Without using it, the measured result could be harder to be obtained since it is unstable. Hence, the properties of Rogers Duroid 6006 are very important in this case.

Not only that, the etching process in fabrication stage might affect the measured result since it is impossible for author to fabricate it perfectly. Any imperfection will deeply affect the measured result. So the stability of the substrate is very important. Any changes of the permittivity of substrate will definitely affect the result and this is the main reason why Rogers Duroid 6006 is chosen as substrate, although we need to spend more. The details will be discussed later.

#### **2.1.1.2 Effective Dielectric Constant**

On one side of the microstrip line is the substrate and air on the top. The dielectric constant of the substrate ( $\epsilon_0=6.15$ ) will be different than that of the air ( $\epsilon_0=1$ ) and it leads the existence of effective dielectric constant. The electromagnetic wave carried by a microstrip line exists partly in the dielectric substrate and partly in the air above. So, the wave is considered to be travelling in an inhomogeneity medium. This behaviour is commonly described by starting the effective dielectric constant of the

microstrip line. So the effective dielectric constant is just like an equivalent dielectric constant of an equivalent homogeneous medium.

Normally, the effective dielectric constant will be around 50%-85% of the substrate dielectric constant; it depends on the geometry of the microstrip. The phase velocity of the electromagnetic wave on the microstrip line is also affected by it.

The maximum value of the effective dielectric constant is affected by the width of microstrip line. In fact, wider transmission line will get higher value of effective dielectric constant because nearly all of the electric field lines will be concentrated between the metal planes in a wide microstrip line. Lesser effective dielectric constant will be obtained in the narrower transmission line.

For wide transmission line,

$$\text{Maximum } \epsilon_{eff} = \epsilon_r$$

For narrow transmission line,

$$\text{Minimum } \epsilon_{eff} = 0.5 (\epsilon_r + 1)$$

Hence there is a range value of effective dielectric constant where

$$0.5 (\epsilon_r + 1) \leq \epsilon_{eff} \leq \epsilon_r$$

However, there is a general formula to calculate the effective dielectric constant,

When  $\left(\frac{W}{H}\right) < 1$

$$\epsilon_e = \frac{\epsilon_r + 1}{2} + \frac{\epsilon_r - 1}{2} \left[ \left\{ 1 + 12 \left(\frac{H}{W}\right) \right\}^{-0.5} + 0.04 \left\{ 1 - \left(\frac{W}{H}\right) \right\}^2 \right]$$

When  $\left(\frac{W}{H}\right) \geq 1$

$$\epsilon_e = \frac{\epsilon_r + 1}{2} + \frac{\epsilon_r - 1}{2} \left[ 1 + 12 \left(\frac{H}{W}\right) \right]^{-0.5}$$

The  $\frac{W}{H}$  stated in equation above is the ratio of the width to the height of the microstrip line.

The effective dielectric constant problem will not arise in the CAD program's simulations because HFSS simulation software already considered this factor in the simulation. It means that HFSS will automatically convert the substrate dielectric constant into effective dielectric constant during the simulation process in order to obtain optimal practical result. So, simulated results obtained already included the factor of effective dielectric constant.

### 2.1.1.3 Characteristic Impedance

Characteristic impedance is the ratio of the amplitudes of a single pair of voltage and current waves propagating along the microstrip line in the absence of reflections. It acts like a resistance where power generated by a source on one end of an infinitely long lossless transmission line is transmitted through the line but it is not dissipated in the line itself. The general expression for the characteristic impedance is as shown below:

$$Z_0 = \sqrt{\frac{R + j\omega L}{G + j\omega C}}$$

where  $R$  is the resistance per unit length,

$L$  is the inductance per unit length,

$G$  is the conductance of the dielectric per unit length,

$C$  is the capacitance per unit length,

$j$  is the imaginary unit

$\omega$  is the angular frequency

In the microstrip transmission line, the characteristic impedance,  $Z_0$  is also a function of height ( $H$ ) and width ( $W$ ) of the transmission line. It has different solutions depending on the value of  $W/H$ . The characteristic impedance of microstrip transmission line can be calculated using:

When  $\left(\frac{W}{H}\right) < 1$

$$Z_0 = \frac{60}{\sqrt{\epsilon_{eff}}} \ln \left( 8 \frac{H}{W} + 0.25 \frac{W}{H} \right) \text{ (ohm)}$$

When  $\left(\frac{W}{H}\right) \geq 1$

$$Z_0 = \frac{120\pi}{\sqrt{\epsilon_{eff} \times \left\{ \frac{W}{H} + 1.393 + \frac{2}{8} \ln \left( \frac{W}{H} + 1.444 \right) \right\}}} \text{ (ohm)}$$

The value of  $Z_0$  can be calculated using the formula above. In other words, the value of  $Z_0$  can be controlled by changing the value of  $W$ ,  $H$  and  $\epsilon_{eff}$ . In fact, the value of  $Z_0$  is very important because it will affect the reflection loss,  $S_{11}$ .

$$S_{11} = \frac{Z_{in} - Z_o}{Z_{in} + Z_o}$$

The reflection loss,  $S_{11}$  is the loss of signal power resulting from the reflection caused at a discontinuity in a transmission line. This discontinuity can be a mismatch with the terminating load or with a device inserted in the line. Ideally,  $S_{11}$  should be as low as possible since it is not good in the transmission line. Given that  $Z_{in}$  value is fixed, so only  $Z_0$  value can be modified to control  $S_{11}$  value. In order to minimize the  $S_{11}$  into zero and become a matched two port, the  $Z_0$  should be set as same value as  $Z_{in}$ . In this experiment stage, the input impedance will be the Vector Network Analyzer (VNA) connector input impedance. Most of the input ports are designed at 50ohm. In order to prevent any reflections, the  $Z_0$  of microstrip lines should be designed as 50ohm accurately.

The  $Z_0$  can be controlled by modifying the  $W$ ,  $H$  and  $\epsilon_{eff}$ . However, the value of  $H$  and  $\epsilon_{eff}$  are already fixed for the substrate and thus cannot be changed. So, the author can only change the value of width,  $W$ . In fact, using different value of  $W/H$  will obtain different value of  $Z_0$ , as shown in Figure 2.3 and Figure 2.4.

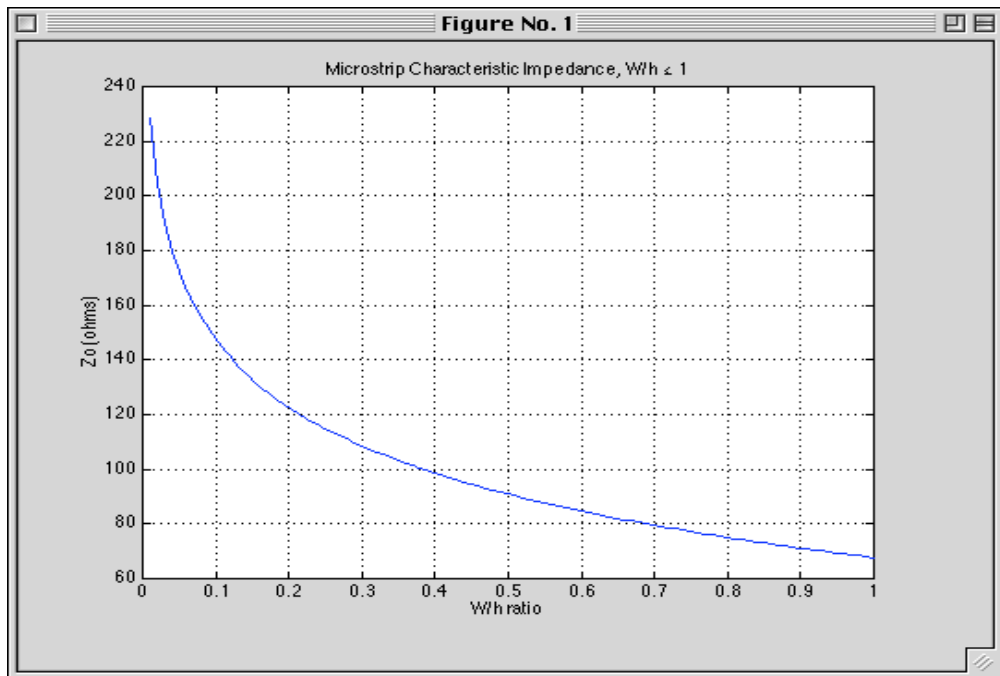


Figure 2.3: Effect of W/H on  $Z_0$  in case  $W/H \leq 1$

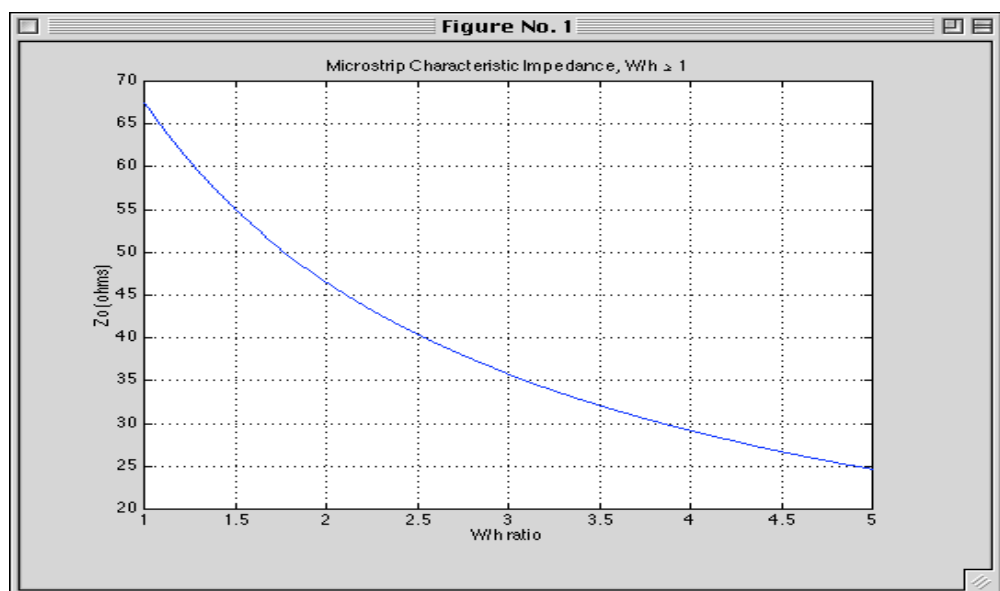


Figure 2.4: Effect of W/H on  $Z_0$  in case  $W/H \geq 1$

However, the formula above is very complicated. The author needs to substitute different value of W in order to obtain the  $Z_0$  value as 50ohm. Software TX Line 2003 solved this problem. It is an useful software. The author just needs to key in the value of width of transmission line, height of substrate, microstrip line thickness and dielectric constant of the substrate (TX Line 2003 will automatically

calculate and use the effective dielectric constant). The software then will calculate the value of  $Z_0$ . This allows the author to modify the value of microstrip line width easily in order to get the  $Z_0$  as 50ohm.

#### 2.1.1.4 Wavelength/ Wave Velocity

Generally, the phase velocity of electromagnetic waves on the microstrip line is determined by the effectiveness of dielectric constant.

The velocity of waves is at  $3 \times 10^8 \text{ms}^{-1}$  in an air spaced microstrip line. The wavelength can be calculated after knowing the value of frequency by formula:

$$\text{Wavelength} = \frac{\text{Velocity of waves}}{\text{Frequency}}$$

Hence, the wavelength on the nominally air spaced microstrip line will be 3cm if it is transmitting in 10GHz of frequency.

However, this formula cannot be applied in calculating the wavelength on the microstrip line because the microstrip is not immersed in a single dielectric. On one side there is a board dielectric and air on the top. So the effective dielectric constant value is needed to calculate the wavelength by the following formula:

$$\text{Wavelength} = \frac{\text{Wavelength on air spaced microstrip}}{\sqrt{\text{effective dielectric constant}}}$$

So in the above example, the wavelength will be  $\frac{3}{\sqrt{7}} = 1.13\text{cm}$ , if the effectiveness of dielectric constant is 7.

Again, the HFSS simulation software considers the effect of effectiveness of dielectric constant when calculating the wavelength. It is one of the powerful features

of HFSS simulation software whereas more accurate simulated results will be obtained.

## **2.2 Dual-mode Microstrip Filter**

The first planar dual-mode filter was proposed in the early 1970's by Wolff and it has recently gained attention in the design of low cost and high-quality filters for a new generation of satellite and wireless communication systems. An essential breakthrough to a low-mass filter design was achieved by the development of the dual mode technique. The introduction of this technique has led to a mass and size reduction by 50% compared to previous used single-mode filters.

The dual-mode concept is stemmed from a physical coupling of two degenerate resonant modes in a geometrically symmetrical resonator such as patch resonator. The coupling of the two modes is achieved by introducing a perturbation element behind the plane of resonator. Thus far, research effort has been invested into experimental and theoretical studies of planar dual mode filters with a cavity-back suspended. These resonators are known to have advantageous features such as size compactness, low radiation loss, and easy-to-design layout because transmission-line theory and design-tools can easily be exploited.

## **2.3 Cavity resonator**

Various patterns of cavity resonators can be found in internet. Prior to the design process of microstrip filter, the author downloaded some related journal from IEEE Xplore and conducted some literature studies about the cavity resonators. The microstrip filters' performance depends' on the cavity resonators. Collecting relevant information is crucial before designing the microstrip filter; design the microstrip filter blindly will not gain any knowledge from it.

In fact, cavity is a three-dimensional resonator in which standing wave forms in a given space surrounded by an enclosed boundary. Maxima and minima in electric fields can be spatially found inside a resonating cavity. The resonances can be used for designing various RF components such as filters, power dividers, and baluns.

### 2.3.1 Elliptic Cavity Filter

Earlier designs of single-mode filters were based on coupling schemes in which all of the direct couplings are present. In dual mode designs, this implies on the perturbation of the cavities in order to couple the degenerate modes of the same cavity. More recent solutions show that dual-mode filters based on cross-coupling schemes without intra-cavity couplings are possible.

The author reviewed Smain Amari and Uwe Rosenberg's paper, entitled "Modular Design of Dual-Mode Filters Using Elliptic Cavities". This paper presents a new design of dual-mode filter by using elliptic cavities in waveguide technology.

The journal states that, a similar idea (elliptic cavities) had been proposed by other professionals. However, some drawbacks were found in those published papers, among them are:

- (a) The designs are based on standard coupling schemes which lack the flexibility of a truly modular design.
- (b) Transmission zeros are not generated and controlled individually by dedicated cavities.
- (c) The stopbands of filters shows significant sensitivity to manufacturing errors when a larger number of transmission zeros are required by the specifications.

The authors of this paper mentioned that non-resonating nodes (NRN) used in the designs are able to solve all of the problems. Figure 2.5 shows the layout of a second-order dual mode filter in an elliptic cavity resonator. A Chebychev filter

results when the output is rotated by  $90^\circ$  with respect to the input which is at  $45^\circ$  from the major axis.

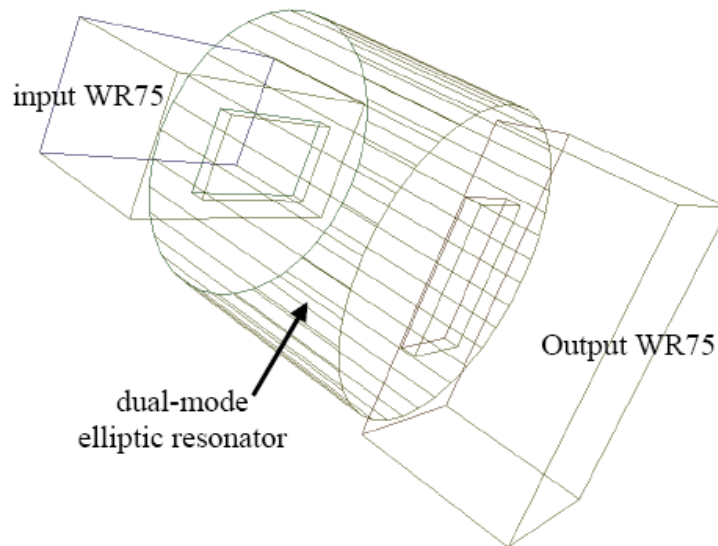


Figure 2.5: Layout of a second-order mode filter in an elliptic cavity resonator.

The major and minor axes of the cross section are 'a' and 'b'. In the limit where  $a=b$ , the elliptic waveguide can support two TE modes which reduce to the degenerate  $TE_{11}$  modes of a circular waveguide. These are denoted by  $TE_{c11}$  and  $TE_{s11}$  respectively. When 'a' is not equal with 'b', the two modes will have different cut-off frequencies and  $TE_{c11}$ ,  $TE_{s11}$  will be different.

Figure 2.6 is the coupling mechanism for dual-mode filters in elliptic cavity resonators. The angle  $\theta$  is used to control the relative coupling to the two modes of the elliptic resonator.

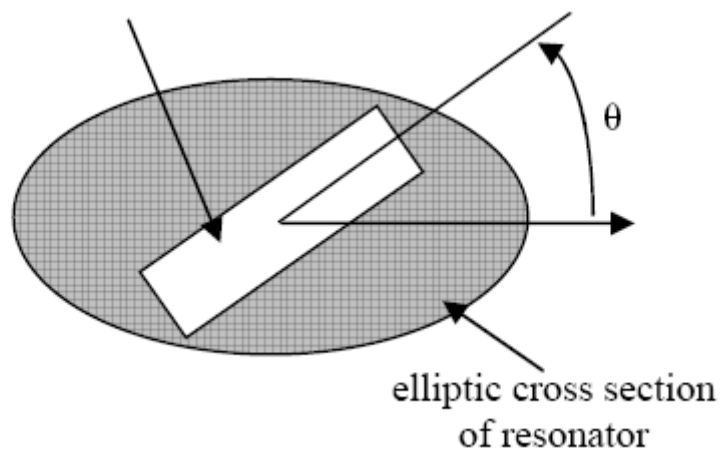


Figure 2.6: Coupling mechanism for dual-mode filters in elliptic cavity resonators.

So, the relative strengths of the coupling coefficients to the  $TE_{c111}$  and  $TE_{s111}$  can be controlled by adjusting the angle  $\theta$  value. For example, if  $\theta = 0^\circ$ , only the  $TE_{c111}$  resonance is excited. On the other hand, when  $\theta = 90^\circ$ , only the  $TE_{s111}$  is excited.

Authors have simulated some result by modifying the angle,  $\theta$ . When the coupling aperture at the input and output are rotated by  $+45^\circ$  and  $-45^\circ$ , Figure 2.7 is obtained whereas two transmission zeros have been moved away from the band.

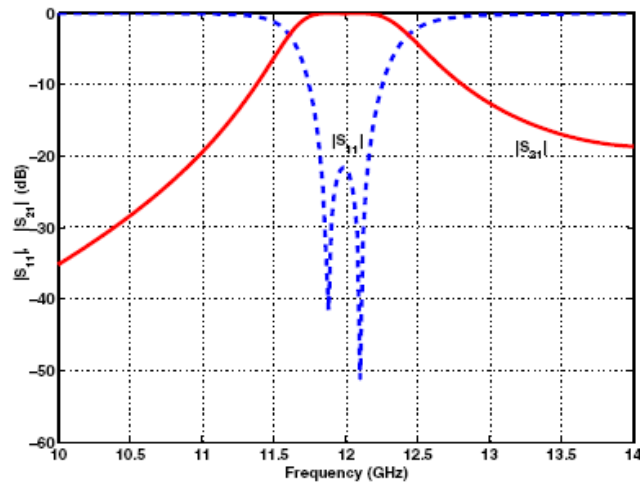


Figure 2.7: Response of a second-order Chebychev filter in a dual-mode elliptic cavity

After that, Figure 2.8 is obtained after adjusting the angle,  $\theta = 36^\circ$  at the input and  $-36^\circ$  at the output where the transmission zero below the passband.

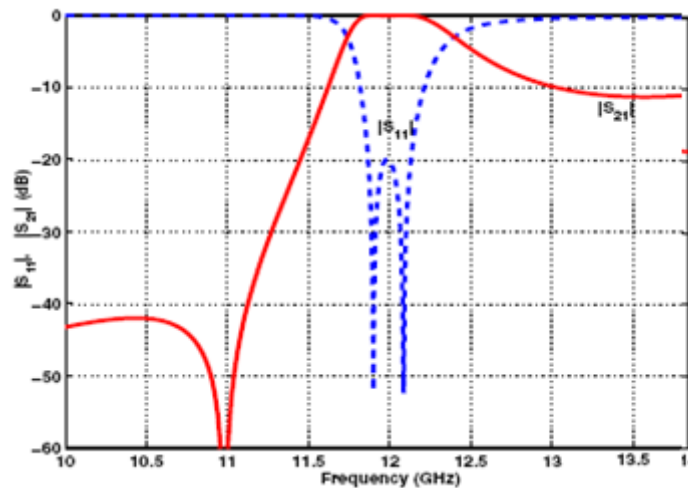


Figure 2.8: Response of a second-order filter with one transmission zero below the passband

Figure 2.9 is obtained in case of the angle at the input are  $52^\circ$  and  $-52^\circ$ . The transmission zero above the passband.

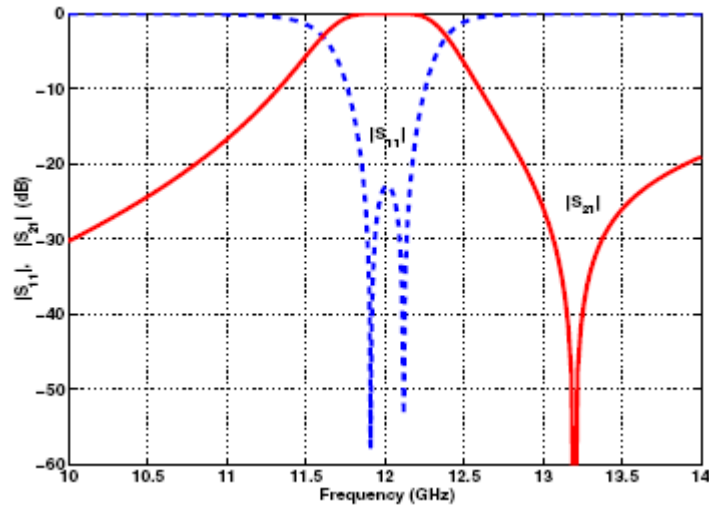


Figure 2.9: Response of a second-order filter with one transmission zero above the passband

In conclusion, this paper presents a new design of filters using dual-mode elliptic cavity resonators. Both filters with Chebyshev characteristic and responses with transmission zeros at finite frequencies can be designed by adjusting the coupling elements between the cavities and the input and output.

### 2.3.2 Square Cavity Filter

The author reviews Da-Peng Wang, Wen-Quan Che and Peter Russer paper, entitled “Tunable Substrate-Integrated Waveguide (SIW) Dual-Mode Square Cavity Filter with Metal Cylinders”. This paper presents a narrow-band substrate-integrated waveguide (SIW) dual-mode square cavity bandpass filter.

In the beginning, authors of this paper discuss about the background of the dual-mode filter. They mentioned that dual-mode filter can be made from the cavity filter, patch filter and microstrip filter. They also listed down all of the advantages and disadvantages of the patch filter, microstrip filter and cavity filter.

The authors reported the dimension used in the design with the SIW width,  $a = 18\text{mm}$ , cylinder spacing,  $W = 1.2\text{mm}$  and cylinder radius,  $R = 0.4\text{mm}$ . Figure 2.10 shows the square SIW resonance cavity.

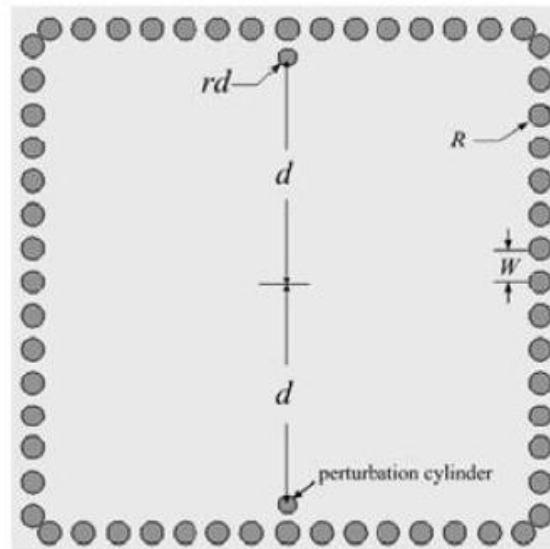


Figure 2.10: Square-SIW resonance cavity

The authors emphasized that there are two modes in the square SIW cavity; these two modes will resonate at the same frequencies by introducing perturbation metalized cylinders. After placing E and H wall at the symmetry plane of the cavity, the E-field distribution of odd mode and even mode appear as shown in figures below. From Figure 2.11 and Figure 2.12, it can be seen that odd mode in the perturbation cylinders are just located at the region where the E field are weak. Meanwhile, the perturbation cylinders are positioned at the region with strong H field at the even mode. Hence the even mode is much stronger than odd mode and it produces the different resonant frequencies. The passband exists due to the different resonant frequencies.

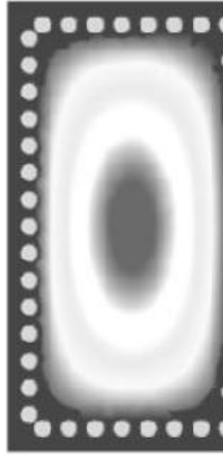


Figure 2.11: Electric-field distribution of odd mode (E wall)

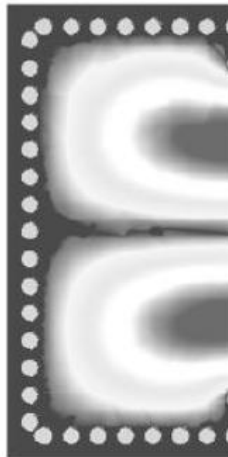


Figure 2.12: Electric-field distribution of even mode (H wall)

Figure 2.13 is the schematic geometry of square SIW cavity dual-mode filter. In this schematic, the chosen distance ( $d_m$ ) between the tuning post and the microstrip line is  $a/4$  (4.5mm). The authors addressed that resonant frequencies of two modes have much dependence on the parameters  $g$  and  $d$ . Figure 2.14 shows the dependence of the resonance frequency of the even and odd modes on the position of the posts.

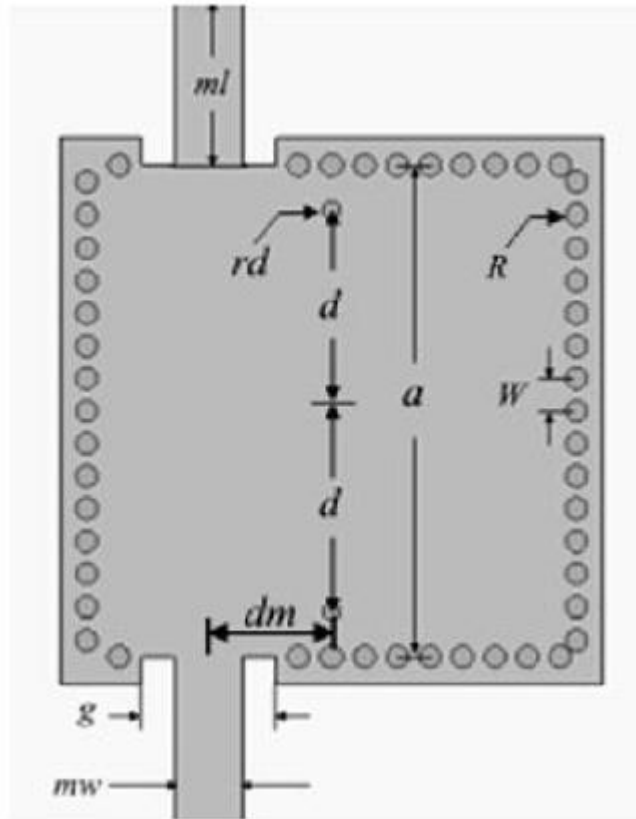


Figure 2.13: Schematic geometry of square SIW cavity dual-mode filter

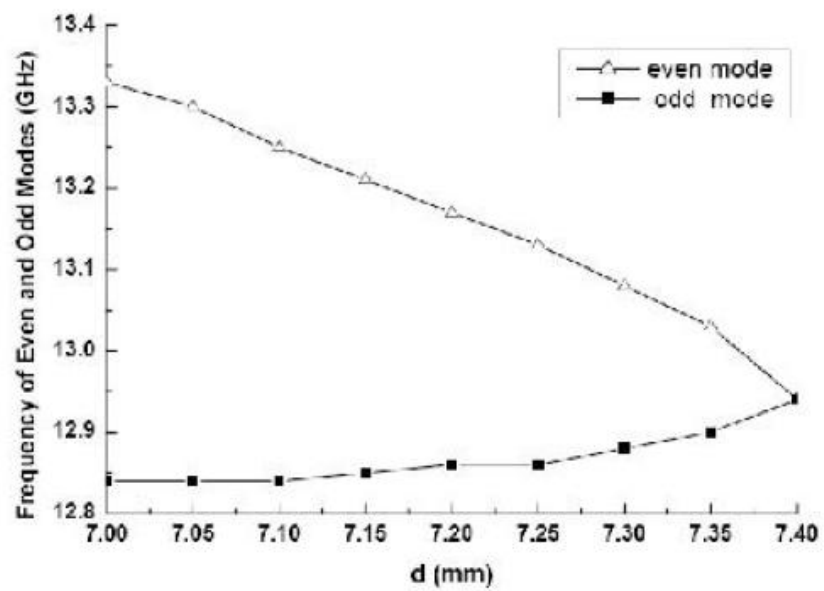


Figure 2.14: Two modes resonant frequencies versus  $d$  (with microstrip Feeding ports)

The authors conducted the simulation using different value of distance between the two tuning post. Figure 2.15 shows the affection of the distance of the two tuning post,  $d$  on the out-of-band rejection.

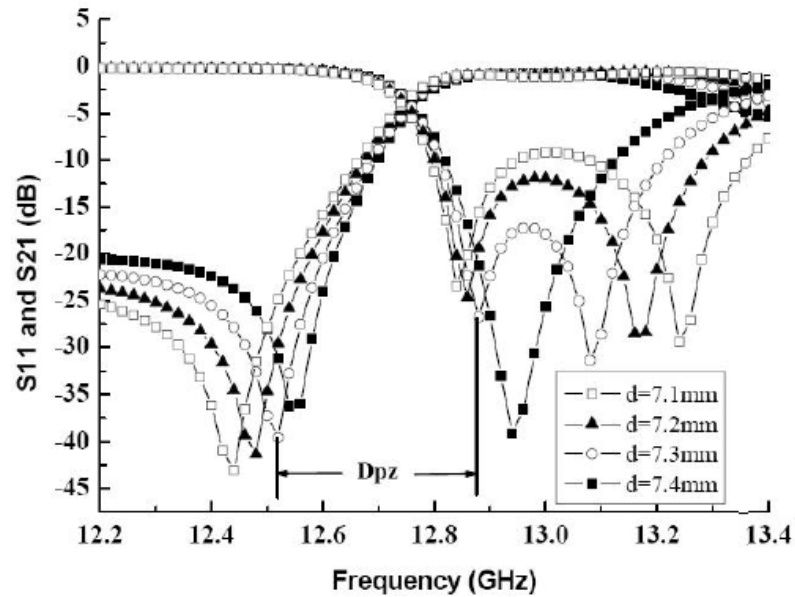


Figure 2.15: Influence of cylinder position in transmission zero and poles

Finally, the authors reported all of the parameters used in design, where the dual-mode filter is fabricated on 0.8mm thick substrate with dielectric constant,  $\epsilon_r$  of 2.2. The dimensions of the cavity are listed as follows:  $a=18\text{mm}$ ,  $W=1.2\text{mm}$ ,  $R=0.4\text{mm}$ ,  $d=7.38\text{mm}$ ,  $rd=0.3\text{mm}$ ,  $ml=6.1\text{mm}$ ,  $mw=2.5\text{mm}$ ,  $g=5\text{mm}$ ,  $dm=4.5\text{mm}$ . Figure 2.16 is the measured results as well as the simulated results, good agreement between them can be observed. The authors also mentioned that there is only minor difference between the simulated and experiment results.

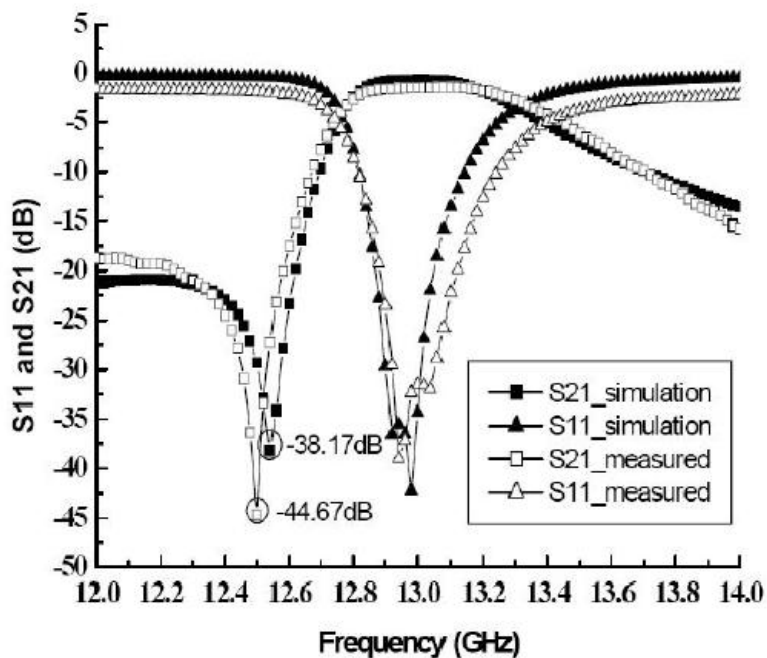


Figure 2.16: Comparison between simulated and measured result

### 2.3.3 Ridge Cavity Filter

The author reviewed Smain Amari and Fabien Seyfert's paper, entitled "Design of Dual-Mode Ridge Cavity Filters". In this paper, a narrow-band substrate-integrated waveguide (SIW) dual-mode square cavity bandpass filter is proposed. They presented variety of dual-mode ridge cavity filters in the paper.

The authors highlighted that they have been various types of dual mode filter designs proposed in the market. The filter designs are mainly based on the theory of Atia and Williams. They are built based on an equivalent circuit which consists of a set of cross-coupled resonators.

The authors stated that coupling schemes used in these filter designs are based on resonances that do not satisfy the boundary conditions inside the dual-mode cavities. This problem is ignored by many for long time. So the coupling elements are introduced in order to solve this problem by altering the original boundary

condition. The coupling elements do not maintain the original symmetry with respect to the horizontal and vertical axes, inside the dual-mode cavity.

The authors decided to build a dual-mode filter using a square ridge with a chamfer in a square cavity. Figure 2.17 shows the symmetry of the resonances that exist in the perturbed cavity.

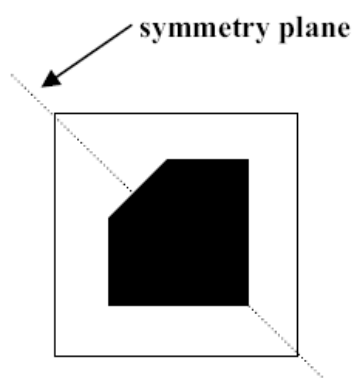


Figure 2.17: Top view of dual-mode ridge square cavity

In the design, the chamfer is used to “couple” two resonances. With the chamfer in place, the resonances that satisfy the boundary conditions have either an electric or a magnetic wall along one of the diagonals. It is impossible for modes with a magnetic or an electric wall along the vertical or horizontal axes to exist in this structure.

The cavity showed in Figure 2.17 can be used to design higher order of dual-mode filters. For example, the fourth order pseudo-elliptic filter which is showed in Figure 2.18.

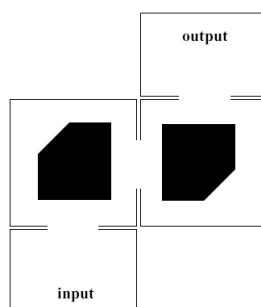


Figure 2.18: Fourth order dual-mode ridge cavity filter

In fact, the authors mentioned that coupling schema in the form of a quadruplet will be different from the present of chamfer. This can be proven in two figures below. Figure 2.19 is the coupling scheme of forth order filter when the vertically and horizontally polarized resonances of the unperturbed ridge cavity are used as basic.

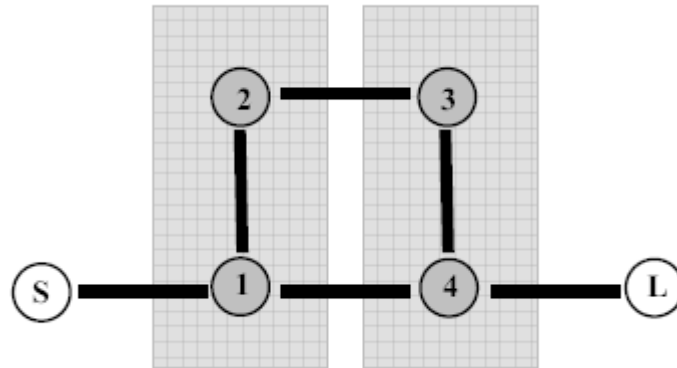


Figure 2.19: Coupling scheme of forth order

If the resonances that satisfy the boundary conditions inside the cavity are used with the chamfer in place, the coupling scheme as shown in Figure 2.20 will be obtained.

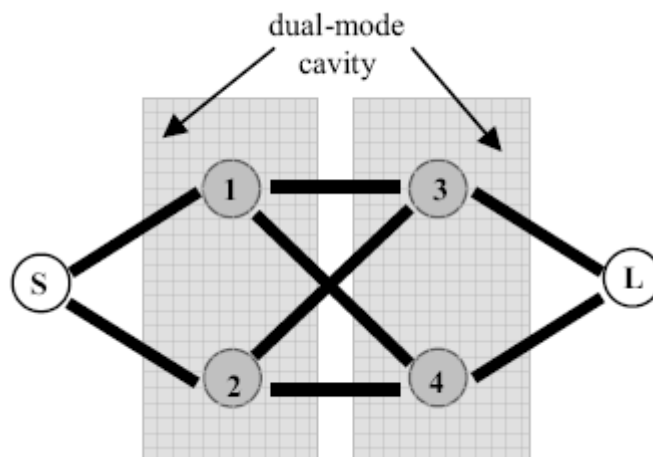


Figure 2.20: Coupling scheme of forth order dual-mode ridge cavity filter when the resonances of the chamfered ridge are used as basic

Authors listed down other possible configurations using the same concept too as shown by the following configurations.

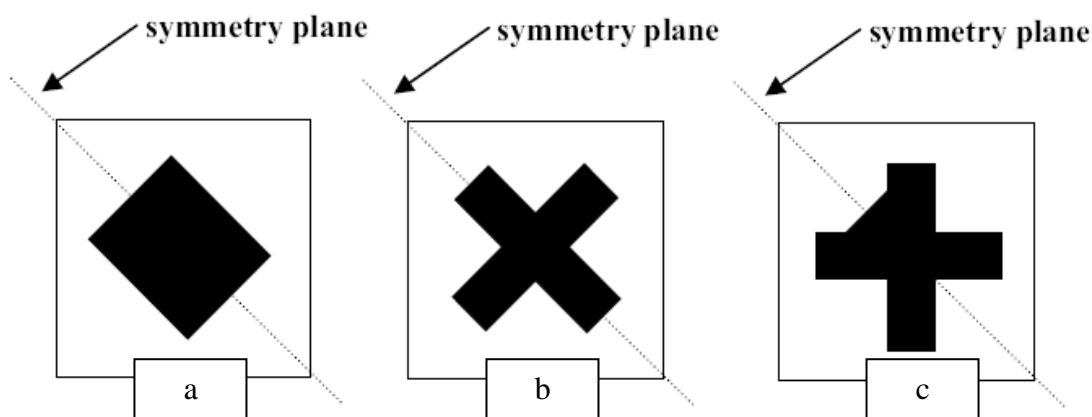


Figure 2.21: Possible ridge configurations for dual-mode filters

Figure 2.21a uses an almost-square ridge whose sides are at  $-45^\circ$  or  $45^\circ$ . The fields in this design are rotated to the proper direction by physically rotating the ridge itself. Meanwhile, Figure 2.21b uses two almost identical arms in the form of a cross hat is also rotated by  $45^\circ$ . In Figure 2.21c, the perturbation which preserves the symmetry along the diagonals of the cavity is used to force the rotation of the fields.

The authors ensure that all of the structure designed will not be symmetric with respect to the horizontal and vertical axes.

The authors chose to extend the investigation of structure in Figure 2.21a for the three new configurations as showed in figures above. Using it, the forth order dual-mode ridge cavity filter with rotated almost-square ridges is build.

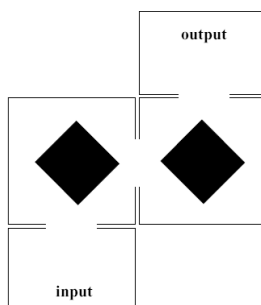


Figure 2.22: Top-view of the layout of the filter.

The filter is optimized by exploiting an efficient rational function approximation technique. Figure 2.23 shows the result of the optimization by simulated using software package CST.

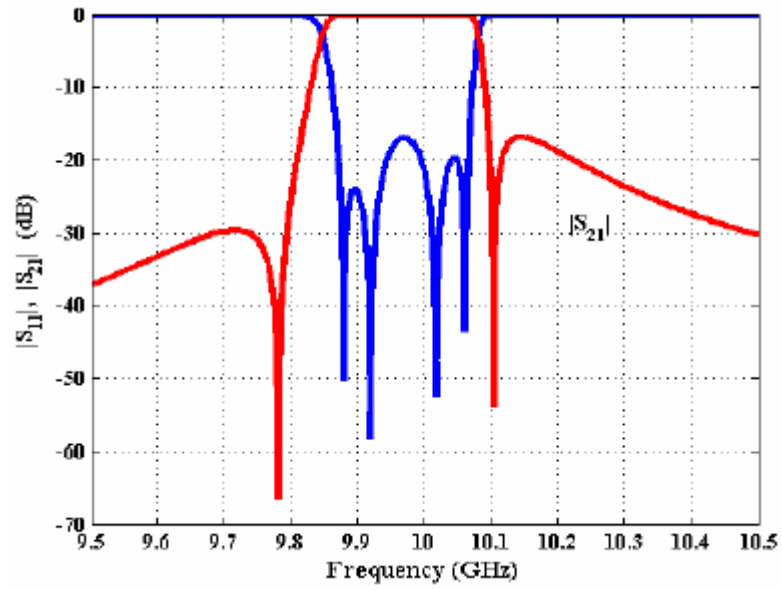


Figure 2.23: Fifth order pseudo-elliptic filter

## CHAPTER 3

### DUAL-MODE MICROSTRIP BANDPASS FILTER

#### 3.1 Background

The fundamental design of the dual-mode microstrip bandpass filter is based on a paper entitled “*Wideband Dual Mode Bandpass Filters with Wide Suppress Harmonics Using Notch Rectangular Slot and Interdigital Coupled Line*” published by Surin Ahonnom and Prayoot Akkaraekthalin. In this paper, a wideband dual-mode bandpass filter was built using a square ring resonator structure. The filter was designed to achieve high harmonic suppression. A perturbation was implemented by a rectangular notch. There, an interdigital coupled line with open stubs is presented. The advantages of the presented bandpass filter include compact size, low insertion loss, sharp rejection, wide stopband, high quality factor, and low cost.

The proposed microstrip bandpass filter is shown in Figure 3.1. It is designed at a fundamental resonant frequency of 5GHz and fabricated on the GML 1000 substrate with a thickness of  $h = 0.762\text{mm}$  and a relative dielectric constant of  $\epsilon_r = 3.2$ . Other parameters are  $I_f = 9.4\text{mm}$ ,  $I_r = 37.54\text{mm}$ ,  $w_1 = 1.8\text{mm}$ ,  $a = 12.085\text{mm}$ ,  $I_t = 9.385\text{mm}$ , and  $w_2 = 1.82626\text{mm}$ . Figure 3.2 tabulates the photograph of the proposed filter. The measured results show that the proposed filter is able to work and function properly. Figure 3.3 shows the comparison between the simulated and experimental result. The measured result verified the theoretical result to the simulated one.

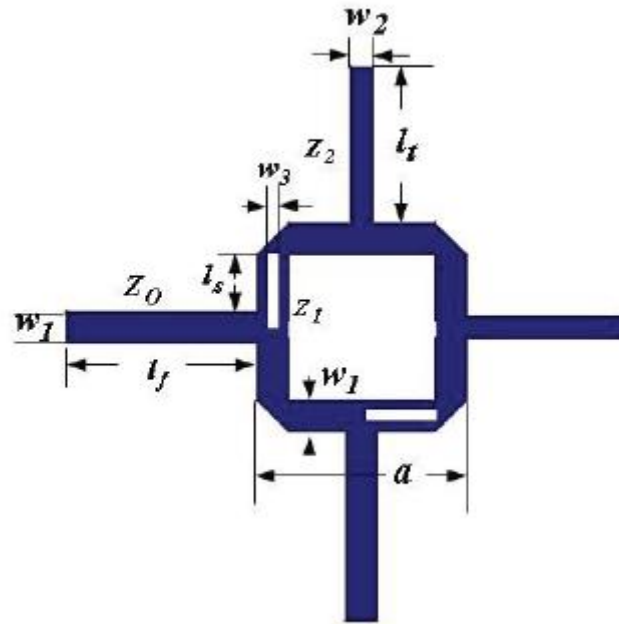


Figure 3.1: Configuration of proposed filter

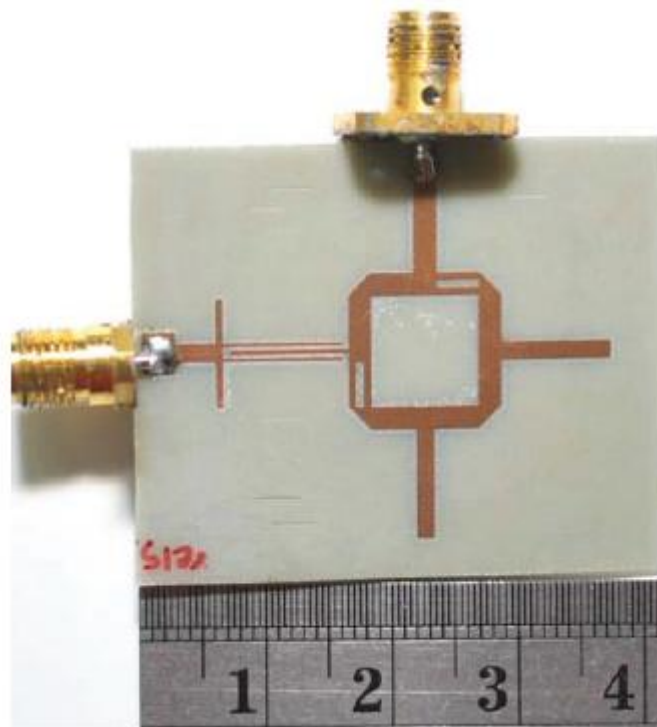


Figure 3.2: Photograph of the proposed filter

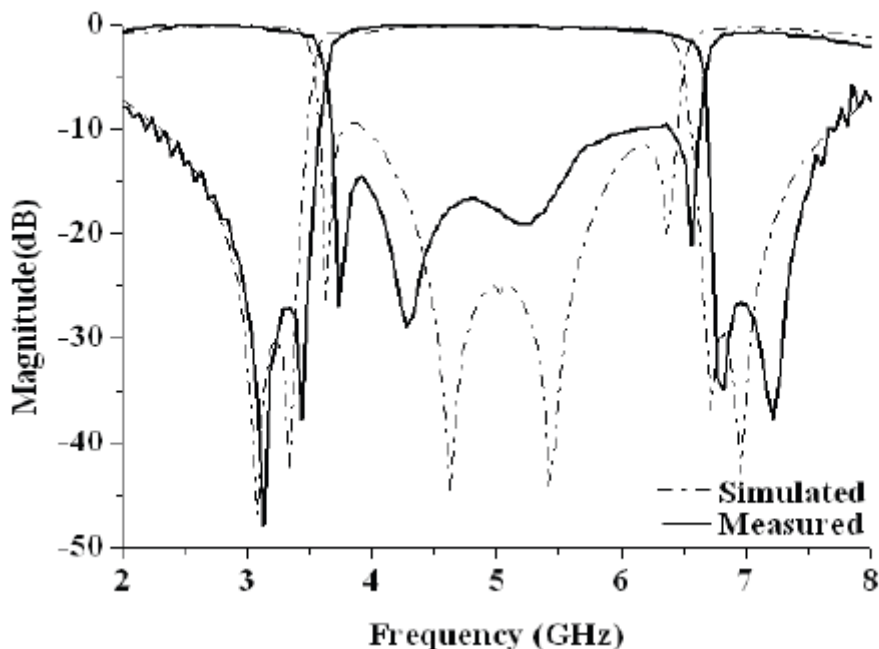


Figure 3.3: Comparison between simulated and measured result

## 3.2 Research Methodology

The reviewed journals are useful for the author to design his filter. The information applied in the reviewed journals can be referred. There are three main stages: simulation stage, fabrication stage, and experimental stage. Different problems arose at different stages. Plenty of time was being spent to solve the problems in order to obtain precise and accurate results. The details are discussed in this chapter.

### 3.2.1 Simulation Stage

HFSS (High Frequency Structure Simulator) and CST Microwave 2009 softwares could be used at this stage. The CST Microwave 2009 is a specialized tool for 3D EM simulations. It enables fast and accurate analysis of high-frequency devices such as antennas, filters, and couplers. It can be used to study the EMI and EMC effects of the planar and multi-layer structures. On the other hand, HFSS is an industry-

standard for 3D full-wave electromagnetic field simulations. It is essential for design of high-frequency and high-speed components. Users only need to specify the geometry and the material properties in order to get the desired outputs. HFSS will automatically generate an appropriate, efficient, and accurate mesh in solving the problem using the proven finite element method.

HFSS is used in this project. It has a higher simulation speed. In fact, CST Microwave 2009 will consume nearly half of a day to simulate a simple filter design. Meanwhile, HFSS needs only few hours to complete a simulation task for a complicated filter design. As both of the softwares are able to produce satisfied results, HFSS is selected due to its shorter simulation time required. Moreover, the simulated result of HFSS is better and more accurate. It improves the quality of proposed filter effectively.

HFSS is new to the author. Several tutorials and practical examples have been studied in order to get himself familiarize with this software. The tutorials entitled “*Ansoft HFSS Training Example: Aperture-Coupled Patch Antenna*” and “*Ansoft HFSS Software Demonstration Example: Microstrip Transmission Line*”. The author needs to follow the instructions and steps listed in order to plot the simulated result. It aims to let the user to get familiarize with the control tools in HFSS. Not only that, a published paper entitled “*Dielectric Resonator Antenna in a Polarization Filtering Cavity for Dual Function Application*” was reviewed. This paper is proposed by Laila, Darko Kaifez and Ahmed A.Kishk. The author plotted the simulated result by using the provided parameter. Some divergences between HFSS and paper simulated results are acceptable because the use of different simulation software might cause results variations.

The author then performed the simulation on his own proposed filter. The prototype of the proposed filter was given by the supervisor. However, it is an immature design and the simulated result is not satisfied. Hence, optimizing the simulated result shall be continued. The result with wider passband and lower power loss is preferred. In reality, the simulation time will be longer when the proposed filter is more complicated. Hence, more time will need to be spent. Eventually, a final version of microstrip bandpass filter configurations has been proposed as in

Figure 3.4. The substrate has a dielectric constant of  $\epsilon_r = 6.15$ . Dimensions of the filter:  $l_1 = 50$  mm,  $l_2 = 20.95$  mm,  $s_1 = 36$  mm,  $s_2 = 30$  mm,  $W_1 = 0.93$  mm,  $W_2 = 5.535$  mm,  $W_3 = 4$  mm,  $W_4 = 1.5$  mm,  $W_5 = 0.5$  mm,  $g_1 = 0.1$  mm,  $d_1 = 5.1$  mm,  $h_1 = 0.635$  mm,  $h_2 = 4$  mm.

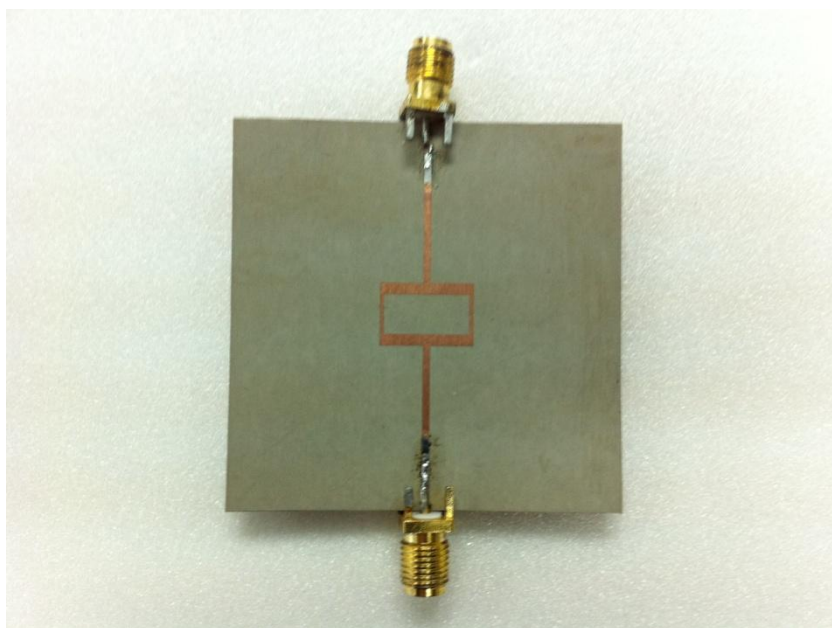
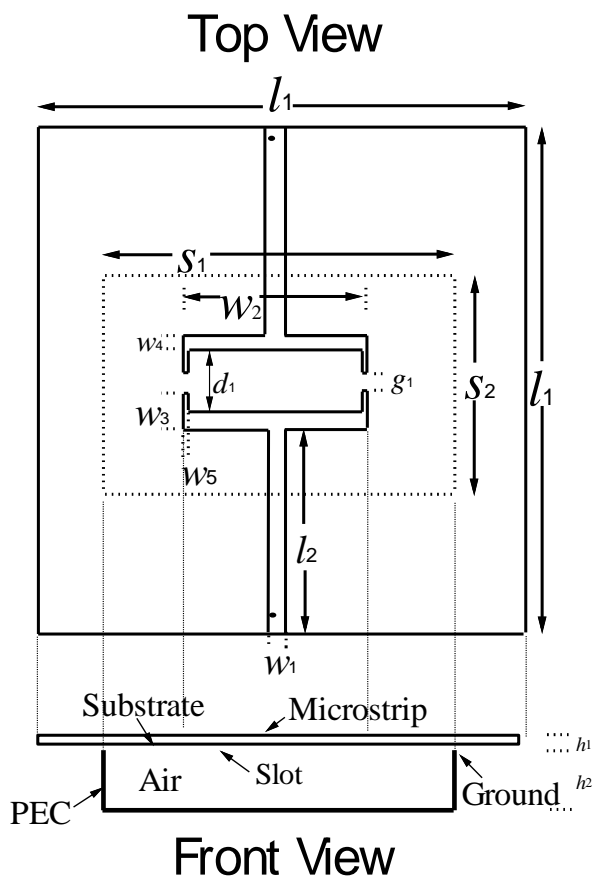


Figure 3.4: Proposed filter configuration

In order to verify HFSS simulated result, AWR Design Environment is used at the simulation stage. In fact, AWR Design Environment is a software that comprises two powerful tools that can be used together to create an integrated system and radio frequency design environment: Visual System Simulator (VSS) and Microwave Office (MWO). These powerful tools are fully integrated in the AWR Design Environment and allow user to incorporate circuit designs into system designs without leaving the AWR Design Environment. MWO enables user to design circuits composed of schematics and electromagnetic structures from an extensive electrical model database, and then generate layout representations of these designs. User can tune or optimize the designs. Meanwhile, VSS enables user to design and analyze end-to-end communication systems. User can design systems composed of modulated signals, encoding schemes, channel blocks and system level performance measurement. Based on the analysis requirements, user can display BER curves, ACPR measurements, constellations, and power spectrums. VSS also provides a real-time tuner that allows user to tune the designs and capture the changes immediately in the data display.

Two different types of simulation software (HFSS and AWR) are used in order to ensure that the simulated result is sufficiently accurate. Both of them use different methods to acquire the simulated result. In fact, the author needs to draw the configuration of proposed filter using the HFSS software. Then, HFSS will process and therefore the simulated result is obtained. Meanwhile, AWR requests author to transform the proposed filter into an equivalent circuit. It means that the substrate, microstrip line and cavity will be replaced by capacitor and transmission line. After that AWR will perform a circuit analysis and get the simulated result.

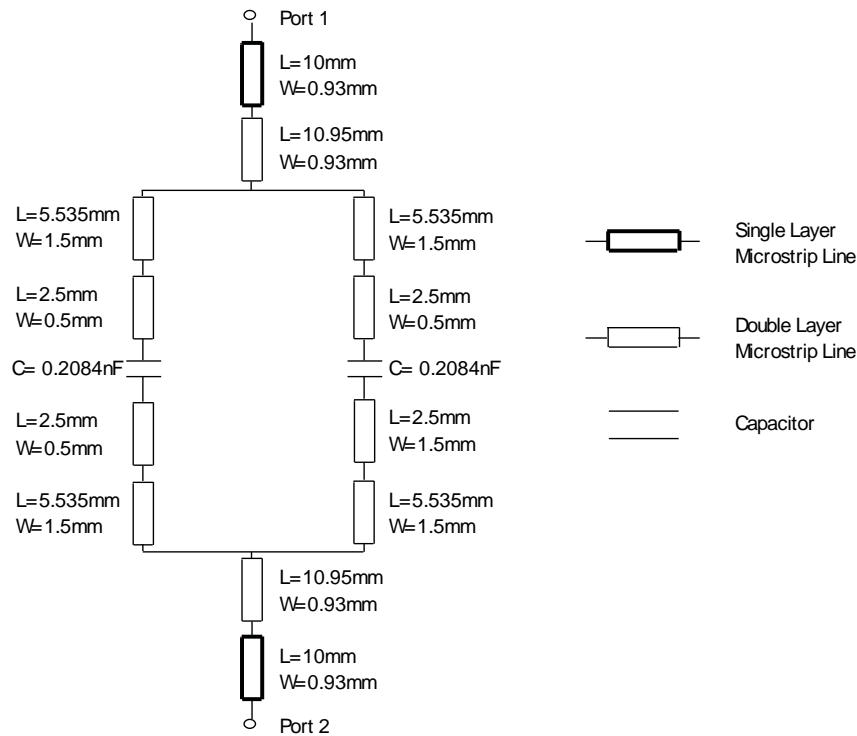


Figure 3.5: Equivalent circuit transformed from the microstrip bandpass filter

### 3.2.2 Fabrication Stage

In this stage, the author fabricated the proposed microstrip bandpass filter. Permission is needed to be obtained from my supervisor in order to proceed into this stage because the materials used to fabricate the filter are very expensive. A 5cm x 5cm of substrate costs around RM100. It is important that the author optimized the simulated result prior to this stage. A small defect in the proposed filter would lead to failure in fabrication and wastage of material. The supervisor would not allow the author to start this stage if the simulation stage is not well prepared. The substrate used is Rogers Duroid 6006 where it costs around RM2000 with just 30cm x 30cm dimension. The dielectric constant of the substrate is 6.15. It is a double sided, photo print and UV negative photoresist material. It is of interest to mention that Rogers Duroid 6006 is a UV negative photoresist material. The details will be discussed later in this study.

In fact, photoresist is a radiation and an ultraviolet (UV) light-sensitive material. For the case of negative photoresist material, the exposed region will become hardened while the unexposed region is removed in the development process. The net result is that the pattern formed is the reverse of the mask. In fact, mask is the pattern the wafer using a UV light source.

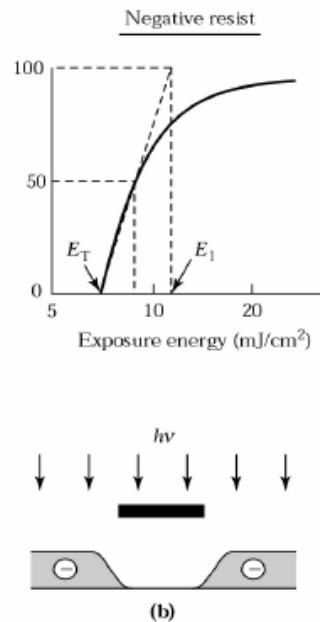


Figure 3.6: Exposure response curve and cross section of the negative resist image after development

Figure 3.7 shows the different IC pattern built using positive and negative photoresist material. It shows the effect of photoresist materials on the fabricated output result (IC pattern). In fabrication stage, the author did the similar job with the figure below, but the output is the microstrip filter but not IC.

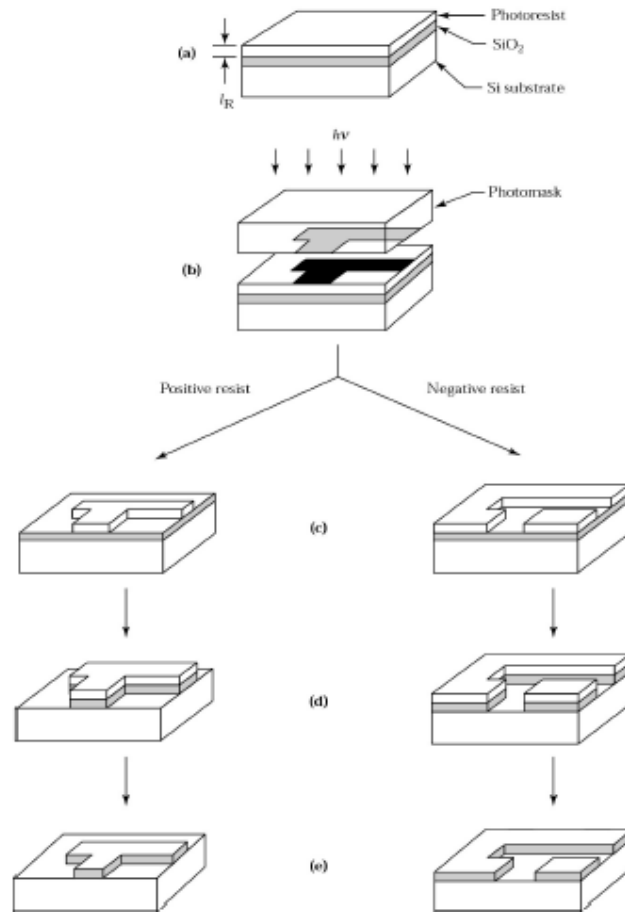


Figure 3.7: Steps to transfer IC patterns from a mask to silicon wafer

Firstly, the author prepared a mask in which needed in fabrication. Tracing paper is used as mask in this project. Filter configuration is printed on the tracing paper using a printer provided in the laboratory. But, the HFSS software does not support printing function, as a result, other printing software is used to draw the filter configuration so that it can be printed on the tracing paper. Exact size of the filter configuration is needs to be printed on the tracing paper because the measured result will be affected even by a 0.1mm mismatch. So an appropriate software have to be used in order to make sure an accurate configuration can be drawn with high resolution. EAGLE (Easily Applicable Graphical Layout Editor) CadSoft is selected. It is a powerful tool for designing printed circuit boards (PCBs). The resolution of EAGLE CadSoft is up to 1/10000mm (0.1micro), so it is sufficient for the author to draw the configuration accurately. Moreover, the filter designed has a cavity attached behind the substrate. It means that the surface under substrate is not totally grounded.

Its shape is also needed to be drawn and printed on the tracing paper. Two tracing papers were prepared.

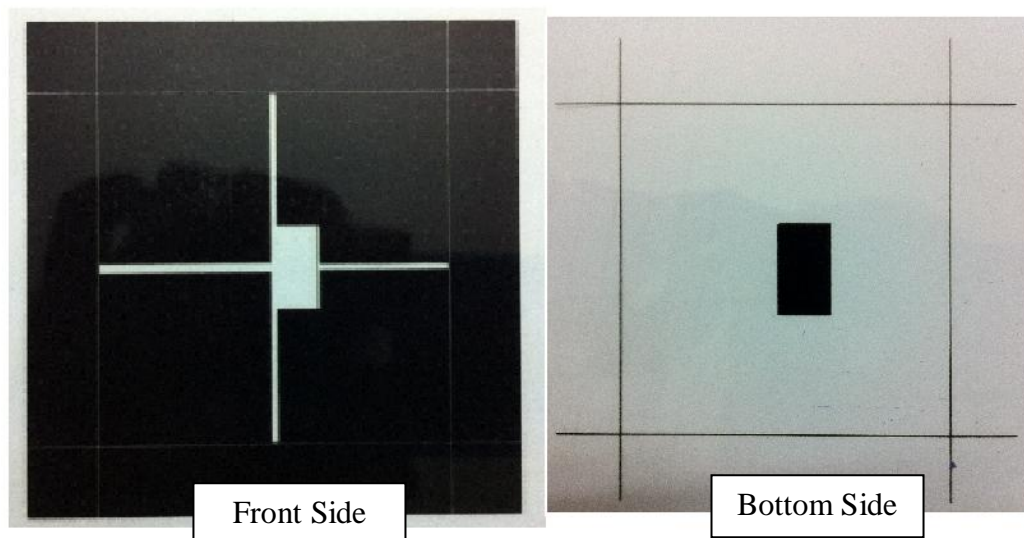


Figure 3.8: Example tracing paper

Secondly is about the pattern transfer. Pattern transfer means that transferring the configuration printed which on the tracing paper to substrate. This process should be performed in a clean room. Only yellow light is allowed to be switched on because photoresists are not sensitive to wavelength of which greater than  $0.5\mu\text{m}$ . In this process, the substrate is aligned with respect to the tracing paper and exposed to the UV light.

Etching process is the next followed by the pattern transfer. It is an important process in fabrication. This process will chemically remove unwanted area from the surface of a substrate. Etching is a critically important process module, and every substrate undergoes etching step before it is complete fabricated. There are two types of etching, which are wet etching and dry etching. However, there is only wet etching which is available in the university. For wet etching, the substrate is dissolved when immersed in a chemical solution. This process requires a container with a liquid solution that will dissolve the material. The unwanted area will be etched after immersed in this chemical solution. The fabrication stage is considered to be done after completing the etching process.

The quality of the board fabricated is very important. As mentioned, even a mismatch of  $0.1\text{mm}$  will caused the measured result at variance. Moreover, the gap

in the filter designed could disappear if this step is not carefully and properly done. It would cause the two isolated microstrip lines to be connected and therefore the fabrication is considered to be failed. In order to avoid the loss financially, the board fabricated is suggested to be reused and recycled. The author can use a penknife to cut a gap on the board, if it is not well fabricated and the gap disappears. It is a step that needed to be highly cautioned because even a small mis-scratch will lead to very different results.

### 3.2.3 Experiment Stage

Experiment stage is the last stage. This stage is to measure the frequency response of the fabricated filter. In this stage, the author needs to install two ports on the board, which are input and output ports. The ports installed connects between the machine and the board. The machine which used to measure experiment result is Rohde & Schwarz ZVB8 Vector Network Analyzer (VNA). The VNA is able to detect the frequency range of any device from 300 kHz to 8 GHz. In the simulation stage, the author knew that frequency range is between 1GHz and 4GHz. Hence, the VNA is appropriate to be used to measure the result.



Figure 3.9: Connector

The VNA cannot be used to detect the experiment result immediately after turning on it. In fact, the author needs to complete a calibration process before measuring the result. Without calibrating the VNA, the result measured might not be accurate. The used of different connector/cable will lead to different phase of signal. Even by removing and installing again the same cable would change the phase of signal. The signal loss might also happen when the cable is changed. The VNA will only be able to self-adjust on the S-parameters after the calibration process. In other words, the main purpose of the calibration process is to eliminate the effect of cable on the measurement. In fact, there are five different ports in the tool kit, which are three single-ports (Open, Short, Match) and one double-port (Thru). In the calibration process, the author needs to connect two ports of VNA with five ports of calibration kit independently. It ensures that the VNA to obtain the most accurate result. The ideal case of calibration is to get the S-parameter as low as possible when connecting to “Match” port of tool kit. However, the environment and equipment variables do not allow it. Hence, the S-parameter which is below 70dB is considered to be satisfied.

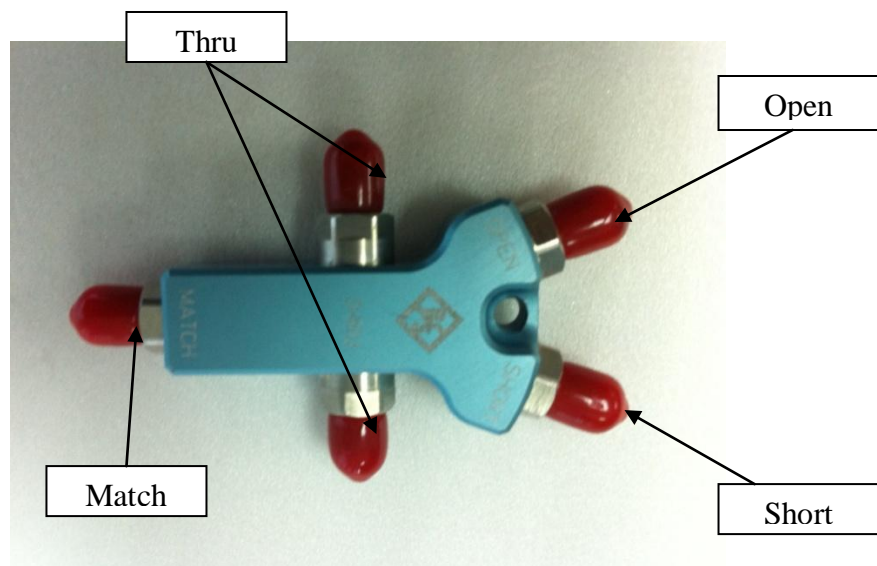


Figure 3.10: Calibration kit

The measurement can be started after the calibration process. In fact, the author needs to connect two cables of VNA with board ports when measuring the experiment result. The frequency range and sweep points have to be set as the same with the simulated result so that the similar measured result with the simulated result

can be obtained. It is of interest to mention that errors occur in the fabrication stage if the measured result is not similar with the simulated result because the simulated result obtained from HFSS is accurate enough and a problem should not be happened therein. However, the author can re-simulate the same configuration for precaution step. If the same simulated result were to be obtained, it then confirms that error happens in the fabrication stage. In this stage, the error might be caused by the improper etching and pattern transfer process. The author might need to re-fabricate a board in order to obtain a measured result which is similar with the simulated result.

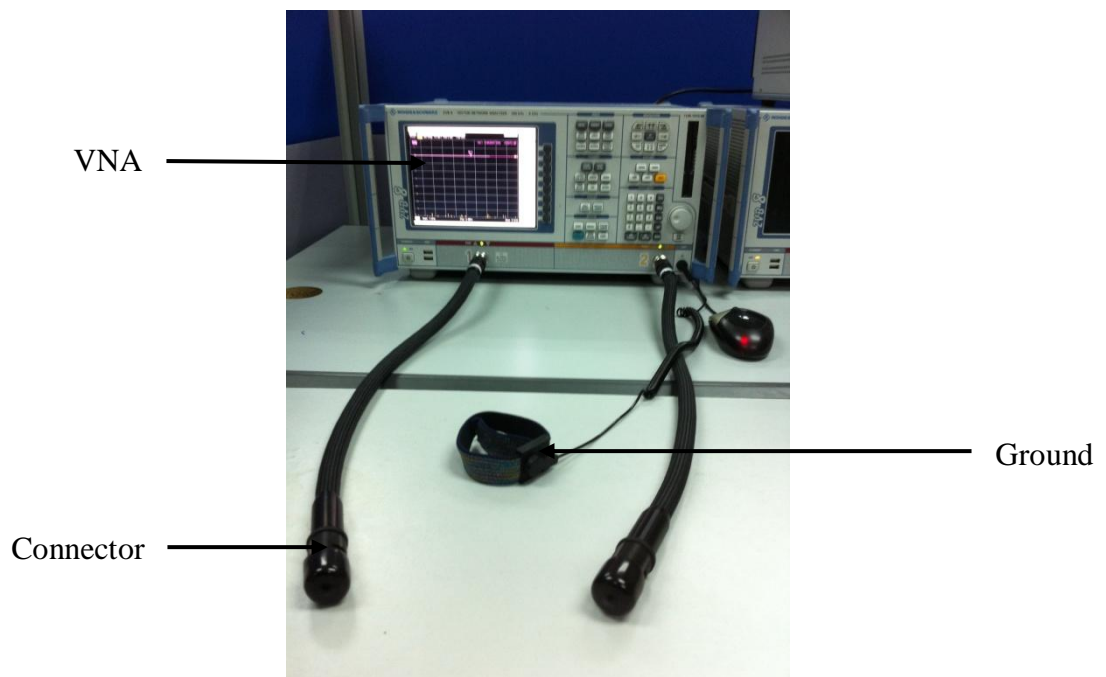


Figure 3.11: Rohde & Schwarz ZVB8 Vector Network Analyzer (VNA).

### 3.3 Proposed Filter Configurations

A dual-mode microstrip bandpass filter was designed based on a cavity-back suspended line. A cavity is attached behind the board and it acts like a resonant. Hence, it can be said that substrate is not a fully ground plane because some area which is covered by the cavity is not grounded. All of the description of the proposed filter configuration is listed in Figure 3.4.

### 3.4 Results and Discussions

All of the measurement result obtained in the experiment stage was performed by Rohde & Schwarz Vector Network Analyzer ZVB8 (VNA). Figure 3.12 shows the comparison between the measured result and the simulation results. In fact there are two simulation results, which are simulated using the HFSS simulation software and AWR simulation software. Figure 3.12 tabulates the graphs of return loss or S-parameter ( $S_{11}$  and  $S_{21}$ ). Although the three different methods used, the results obtained are similar. These three different results verify that microstrip band pass filter designed is working well. The measured result verified well the simulated results.

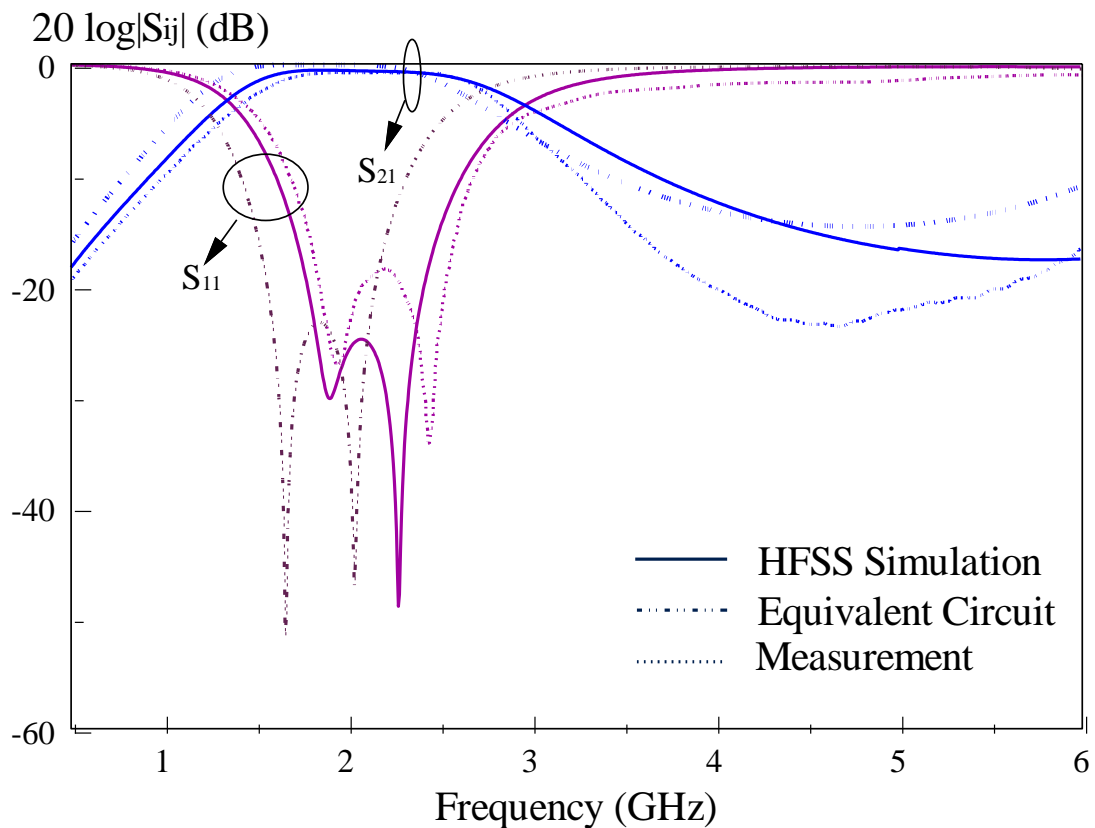


Figure 3.12: Return loss or S-parameter of designed filter

It can be seen that dual-mode microstrip bandpass filter has been designed successfully from Figure 3.12.. It has wide passband (1.42 GHz to 2.84 GHz), low power loss (insertion loss,  $S_{21}$  is very low) and dual-mode property. With the

reference to Figure 3.12, the first order resonance, second order resonance and error between measured and simulated result are calculated.

	Measured	HFSS	AWR	Error (HFSS / AWR)
First Resonance	1.95GHz	1.91GHz	1.67GHz	2.05 / 14.36%
Second Resonance	2.45GHz	2.28GHz	2.04GHz	6.94 / 16.73%

In addition, the central frequency,  $f_c$ , bandwidth and error between the measured and simulated result can be calculated. The results are shown in table below. In fact, the central frequency of a filter is the measurement of a central frequency between the upper and lower cutoff frequencies. Meanwhile, bandwidth is the difference between the upper and lower frequencies in a contiguous set of frequencies. Sometimes, it is referred as the passband bandwidth. The formula to calculate the center frequency, bandwidth and error are as follows.

$$\text{Center frequency} = \frac{\text{Low Frequency, } f_L + \text{High Frequency, } f_H}{2}$$

$$\text{Bandwidth} = \frac{\text{High Frequency, } f_H - \text{Low Frequency, } f_L}{\text{center frequency, } f_c} \times 100\%$$

$$\text{Error} = \frac{|f_c(\text{measured}) - f_c(\text{simulated})|}{f_c(\text{measured})} \times 100\%$$

	Measured	HFSS	AWR
Minimum Insertion Loss (dB)	-0.755	-0.551	-0.081
3-dB Bandwidth (%)	-3.755	-3.551	-3.081
$f_L$ (GHz) / $f_H$ (GHz)	1.42 / 2.84	1.33 / 2.95	1.18 / 2.27
$f_c$ (GHz)	2.13	2.14	1.725
Bandwidth (%)	66.67	75.70	63.19
Error	0.000	0.469	19.014

### **3.5 Case Studies**

The parametric analysis will be presented in this section. The author simulated the proposed filter using a modified parameter. It aims to verify and proves that the values selected in the configuration are able to perform better compared with other values. Same frequency range is used for an easier comparison purpose. Different values of gap distance and cavity dimension are used in order to verify the value used is at the best.

#### **3.5.1 Gap Distance**

Firstly, the author studied the effects of the gap distance on the frequency response. The value of gap distance used in this project is 0.1mm. The two simulated results are showed by replacing the 0.1mm gap distance with 0.3mm and 0.5mm. It can be seen that the gap distance of 0.1mm produces better result from Figure 3.13. The two modes merged together after replacing the gap distance of 0.1mm with 0.5mm. It indicated that the lower value of gap distance is preferred because the smaller gap is able to create a stronger capacitive coupling between the resonators. However, the gap distance which is lower than 0.1mm shall not be used because other problem would arise in the fabrication stage. Due to facility problem, the author could not fabricate out a filter with a gap which is lower than 0.1mm. Hence, a 0.1mm of gap distance is chosen.

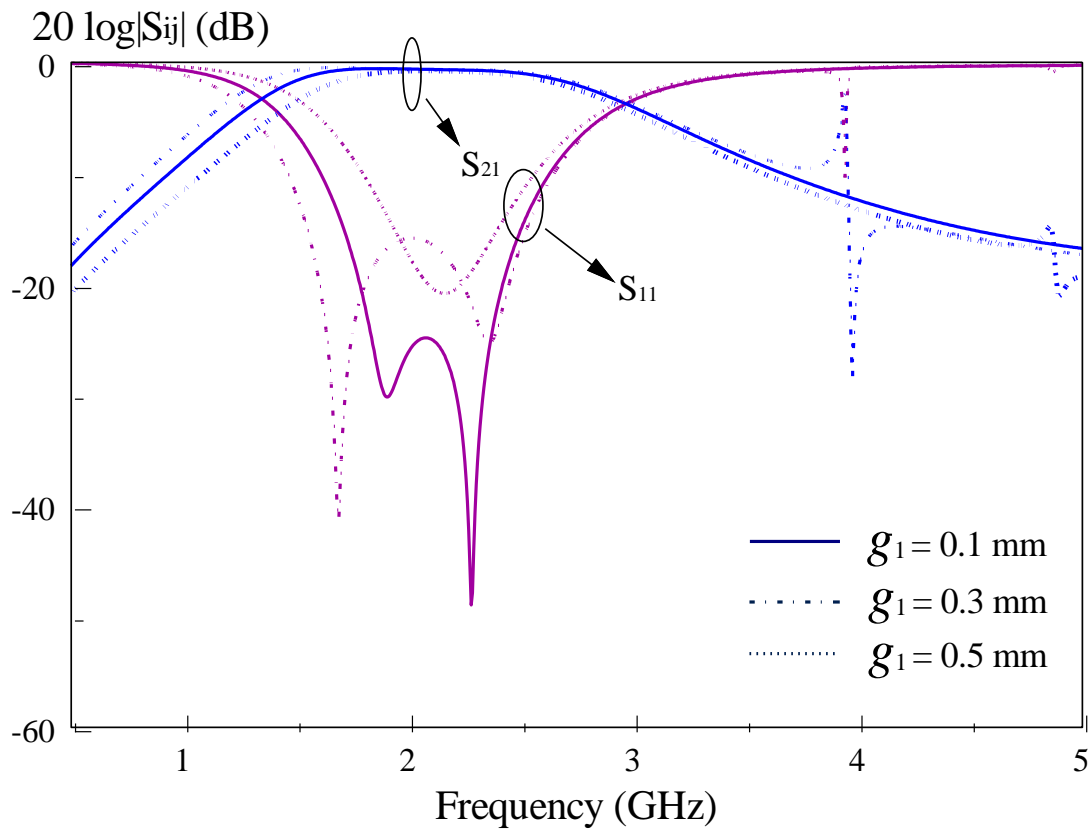


Figure 3.13: Effect of gap distance

### 3.5.2 Slot Dimension

The second issue to be discussed is the size of the cavity. In fact, there are three different dimensions of the cavity, which are height, width and length. Each single change of dimension will affect the simulated result much.

#### 3.5.2.1 Length of Cavity

The length of cavity used in this project is 36mm. After changing into 26mm and 40mm, the simulated results showed in Figure 3.14 are almost the same with the 36mm. In fact, the  $S_{11}$  values obtained are almost the same, which are also lower than -20dB in passband. It indicated that the signal reflected is very low, there is

almost no reflection of signal happened in transmission. Moreover, the three simulated results also showed that  $S_{21}$  values are almost at 0dB in passband. It means that almost all of the input signals have been transmitted from port1 (input) to port2 (output) successfully. By looking at  $S_{11}$  and  $S_{21}$ , the author knows that by changing the different values of the length of cavity will not affect the result so much. Good bandpass filter also can be designed with different values of cavity length. However, cavity length of 36mm is chosen because its  $S_{11}$  value is the smallest in passband.

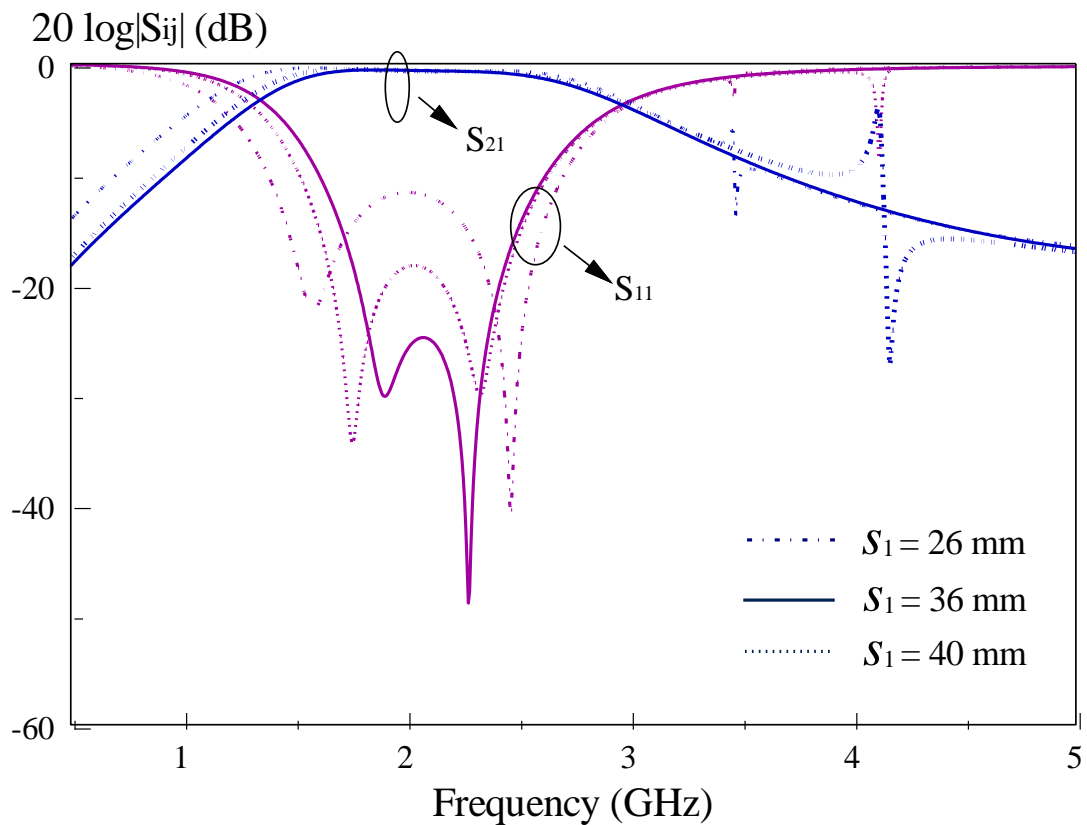


Figure 3.14: Effect of cavity length

### 3.5.2.2 Width of Cavity

The cavity width selected in the present project is 30mm. The performance of the filter is at best by using this value and it can be seen from Figure 3.15. It is undeniable that the passband becomes wider when the width reduces into 24mm. However, there is an additional mode exists between 3GHz and 3.5GHz. The  $S_{11}$  is

unstable and variation happened during that time. Hence, this value cannot be used. Also, when the width of cavity is increased into 40mm, the measured result becomes poorer. The two modes merged together and the passband becomes narrower. Hence, 30mm of cavity width is at used.

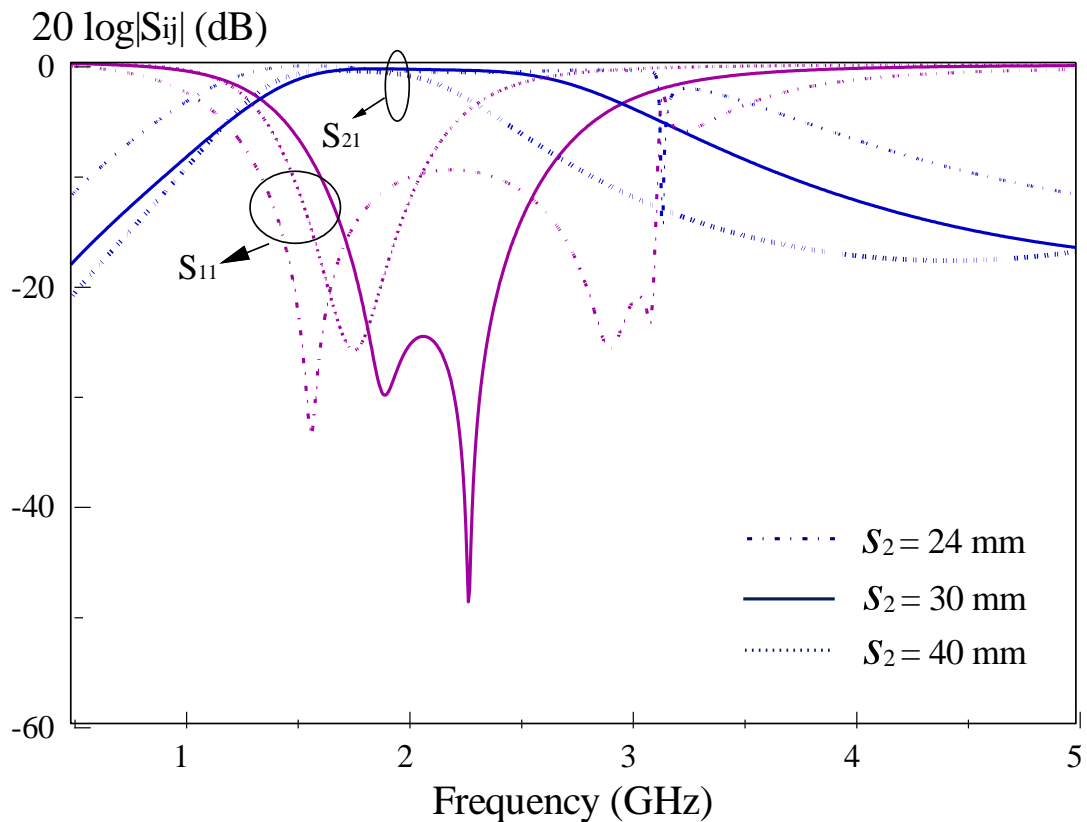


Figure 3.15: Effect of cavity width

### 3.5.2.3 Height of Cavity

The last part of the case study is about the height of cavity. It is the core idea of the present project. In fact, the idea of this project is to design a dual-mode microstrip bandpass filter with a cavity-back suspended line. Obviously, the cavity plays an important role in this project and it can be seen from Figure 3.16. When the author reduces the height of cavity into zero (another way to cancel the cavity), the simulated result shows that the filter designed cannot work well. Without cavity means that the filter designed is unable to work. So, it verifies that the core idea in

this project is correct. Furthermore, increasing the height of the cavity does not bring any benefit, but bad effect instead. The  $S_{21}$  value is not 0dB in passband, but around -2.27dB. It shows that not all signal transmit from the input is received by the output. Signal reflection or leakage might happen during the signal transmission. The formula as shown below indicated that only 77% of input signal is received by output.

$$20\log(P_{out}/P_{in}) = -2.27\text{dB}$$

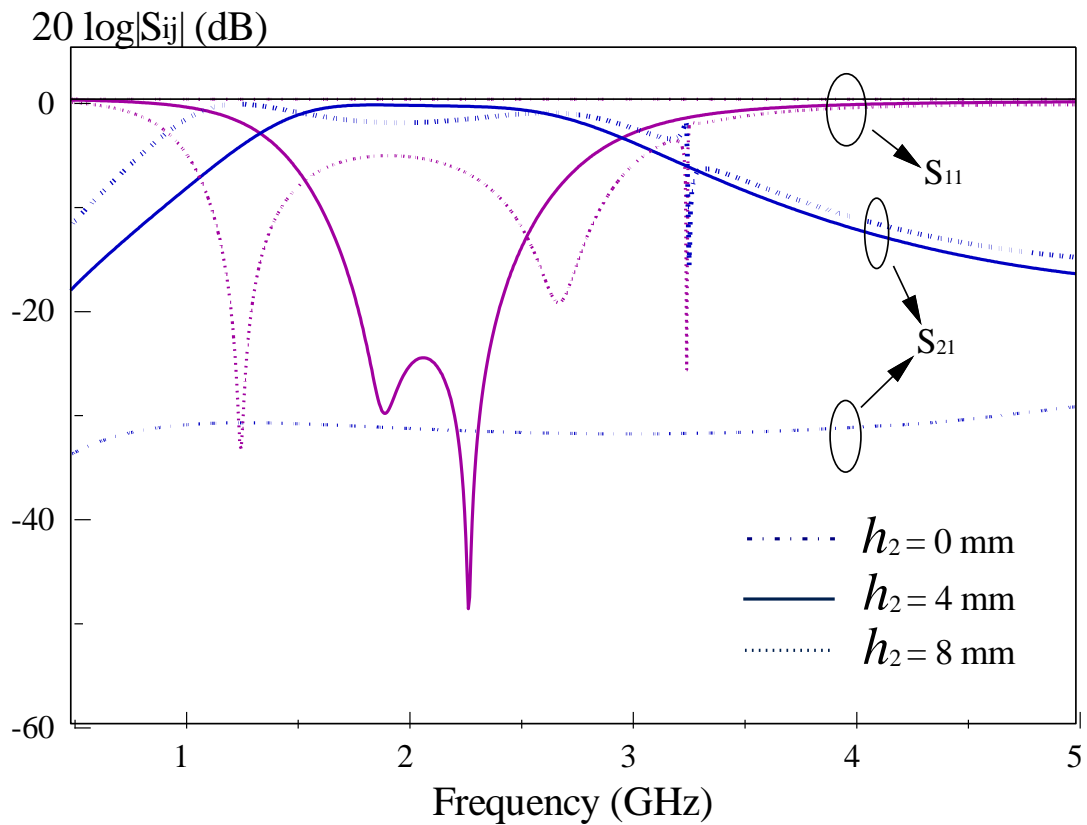


Figure 3.16: Effect of cavity height

## CHAPTER 4

### DUAL-MODE MICROSTRIP POWER DIVIDER

#### 4.1 Background

The fundamental design of the dual-mode microstrip power divider is based on the *Multilayer unequal Microstrip Power divider* by Sheikh S.I. Mitu, SMIEEE, FIET and Sulaiman L. Taiwo. The paper presents a design of a C-band multilayer aperture coupled microstrip power divider.

In the introduction part, the authors of this paper reported that Wilkinson power divider is widely applied in the power divider designed due to its simplicity and high isolation between output ports. However, there is a problem if it is applied in a power splitter which needs high impedance of microstrip line. So, the authors introduced the defected ground structure in the design and it will improve the aspect ratio (W/H).

Figure 4.1 shows the compact aperture coupled two-way microstrip power divider proposed. For the power divider proposed, the dimensions used are:  $L_a=8.25\text{mm}$ ,  $L_b=10\text{mm}$ ,  $W_p=4.5\text{mm}$ ,  $W_s=3\text{mm}$ ,  $L_s=17.7\text{mm}$ ,  $W_{ms}=3.04\text{mm}$ ,  $g=4.9\text{mm}$  and  $t=1\text{mm}$ . The substrate height is 1mm and the dielectric constant is 2.6. The simulated and experiment results reported low insertion loss, high isolation between the output ports and large impedance bandwidth. Moreover, the experiment results agreed well with the simulated result of the power divider.

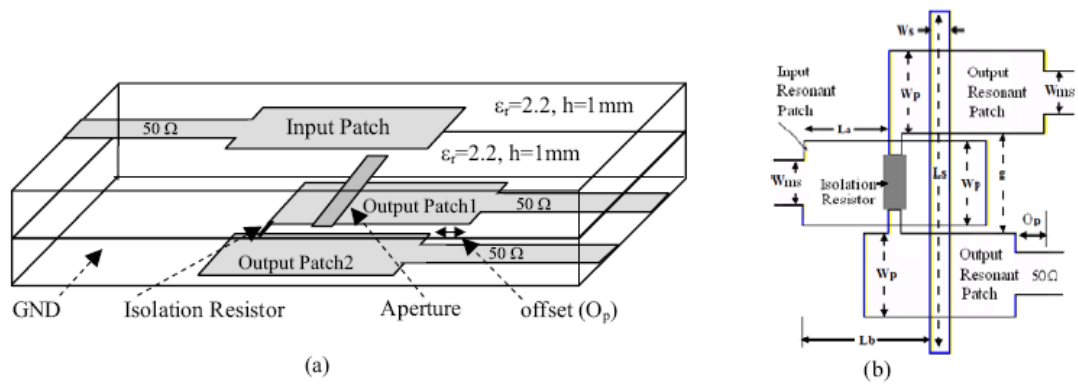


Figure 4.1: (a) 3D, (b) top view of the power divider

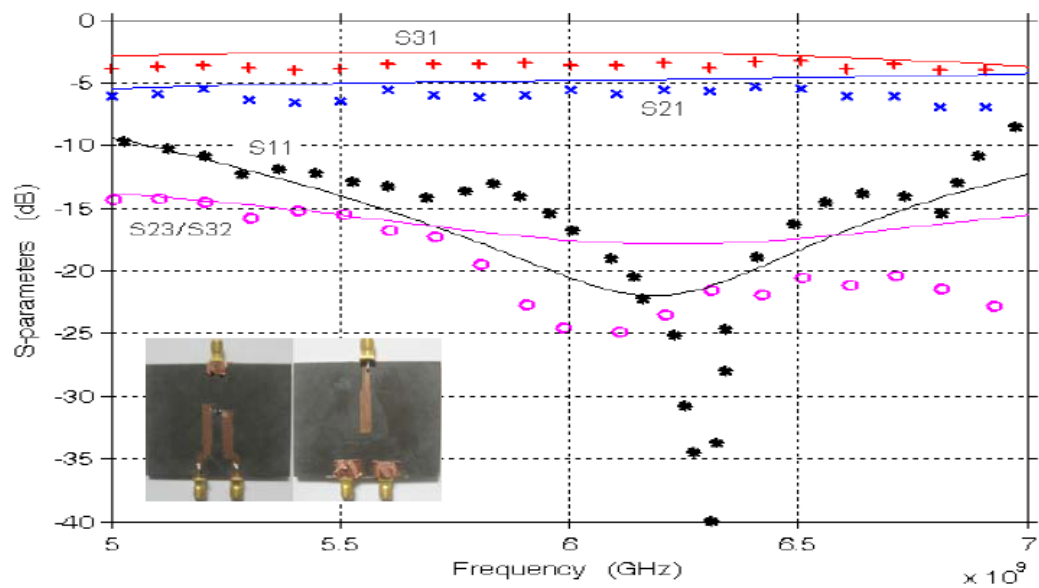


Figure 4.2: Simulated and experimental reflection ( $S_{11}$ ), transmission ( $S_{21}$  and  $S_{31}$ ) and isolation ( $S_{23}$  and  $S_{32}$ ) responses of the power divider

## 4.2 Research Methodology

There are three main stages in designing power divider: simulation stage, fabrication stage and experiment stage. Since most of the parts are similar to the previous methodology, so some repeated information will not be indicated. There is only some additional information will be covered in this chapter.

### 4.2.1 Simulation Stage

Tutorials and practical are not needed in this stage because the same simulation tool, which is HFSS will be used. The author had gotten himself familiar with the overview of HFSS. All of the basic menus, windows, components and commands are well studied. So, the author can start to design his power divider without studying the related tutorials.

The same design procedures are carried on. The supervisor presented a prototype idea of power divider to the author. It is an incomplete configuration of power divider. The simulated result is poor and cannot be used. The author needs to optimize and improve it step by step. Each modification on microstrip line length, width and cavity height, length, width might improve the simulated result. As compared with the simulation stage in the filter design, lesser time is used here because the author has already completed a similar task and has gained the relevant experience needed. The difference between them is just about the number of ports. The power divider has one input and two output ports. Hence, the author needs to be careful when simulating the power divider because the more ports means the more complicated the configuration will be. A same transmission response ( $S_{21}$  and  $S_{31}$ ) should be obtained and balance is very important. Equivalent of output signal strength shall be received from the two output ports. Optimization has to be carried on when signal strength received by two outputs are at variance.

A final version of microstrip power divider configurations has been proposed as in Figure 4.3. The substrate shows a dielectric constant of  $\epsilon_r = 6.15$  and dimensions of the power divider:  $l_1=50$  mm,  $l_2=20.95$  mm,  $l_3=36$  mm,  $l_4=30$  mm,  $l_5=0.93$  mm,  $l_6=5.535$  mm,  $l_7=4$  mm,  $l_8=1.5$  mm,  $l_9=0.5$  mm,  $g_1=0.1$  mm,  $g_2=5.1$  mm,  $w_1=0.635$  mm,  $w_2=4$  mm,  $w_3=50$  mm,  $w_4=20.95$  mm,  $s_1=36$  mm,  $s_2=30$  mm,  $h_1=0.93$  mm,  $h_2=5.535$  mm.

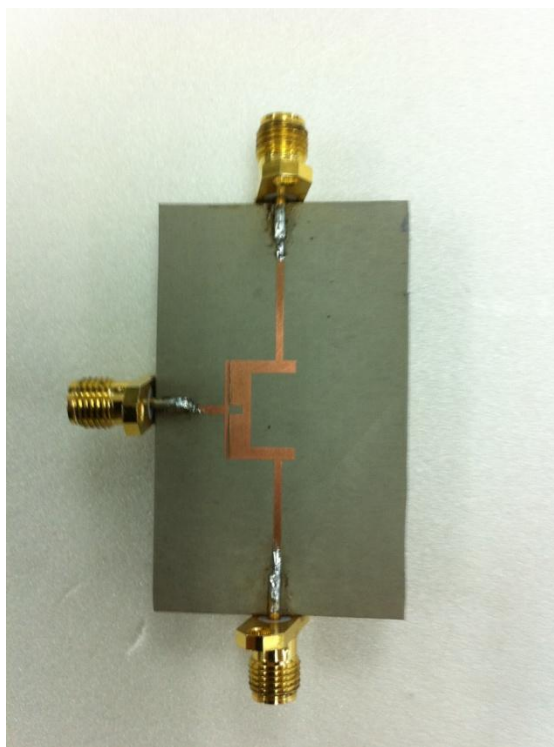
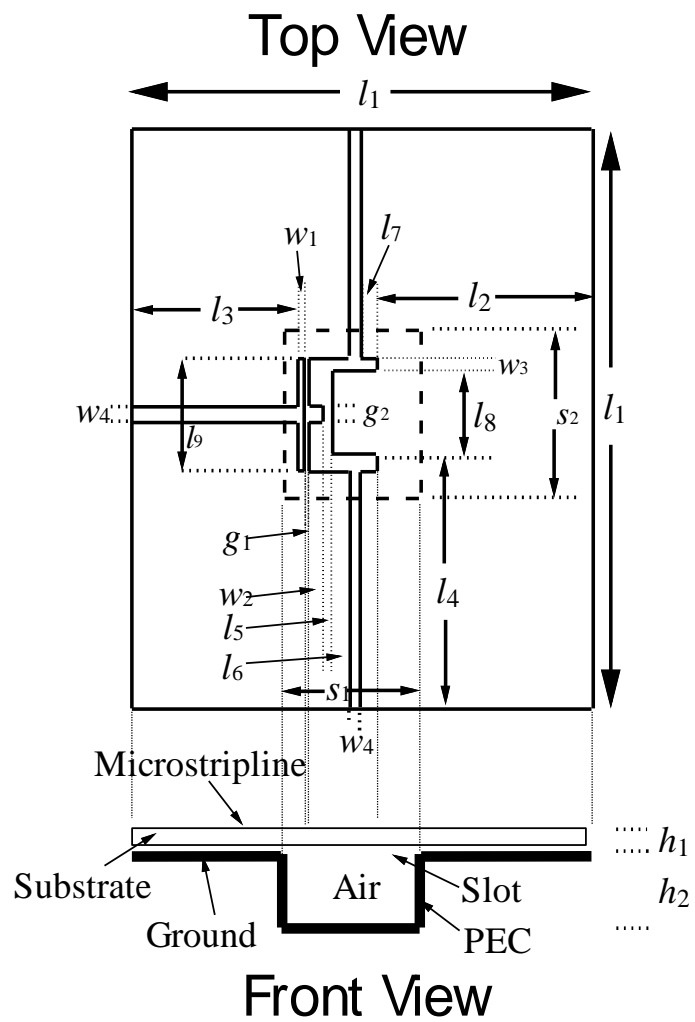


Figure 4.3: Configuration of proposed power divider

#### 4.2.2 Fabrication Stage

Rogers Duroid 6006 is still the substrate that been used. As mentioned, the cost of substrate is very high. Permission from the supervisor is needed to proceed into this fabrication stage. Only power divider that is able to produce excellent simulated result will be fabricated. The substrate that used in this project which is Rogers Duroid 6006 is not available in Malaysia market. Hence, the author have to order the board from the Rogers Head Quarter in Connecticut, USA.

The same work with the fabrication stage in filter design is completed here. First is to draw the power divider configuration using EAGLE CadSoft. Next, print it on a tracing paper. There is a cavity attached under the board, so it is only considered to be partially grounded. The two tracing papers which contained upper and lower sides printed configuration are needed. More precaution steps shall be carried in this project because the complexity and difficulty in fabricating power divider are larger than filter. The length of the power divider is the key point. In fact, the gap length of power divider,  $l_9$  (0.5mm) is larger than filter,  $W_5$  (12.1mm). Although the gap distances of the filter and the power divider are also 0.1mm; the length of gap is different. As mentioned, 0.1mm gap distance is hard to be fabricated. The penknife can be used on filter fabrication because it has only 0.5mm of gap distance. The human error can be avoided but it is a different case for the power divider's gap. A 12.1mm of a gap distance is very long, human error might be unavoidable and it would destroy the fabricated board. The measured result will be affected. So the penknife cannot be applied here. As a result, the author can only rely on his fabrication skill when fabricating the power divider board. In fact, the author spends 3 days to complete the filter's fabrication and experiment stages, but 2 weeks on the power divider's fabrication and experiment stages! This indicated that fabricate power divider is harder than filter. As stated, even a 0.1mm of mismatch will alter the measured result. So, the gap distance of the power divider raised the difficulty in the fabrication stage.

Not only that, the author needs to confirm that higher resolution of configuration is printed on the tracing paper. It is another factor that might affect the measured result. If the printed configuration is blurred and not clear, surely the

pattern transfer process will not be proceeded successfully. The BITMAP file shall be selected as its resolution is higher as compared with other file type. Compare with the fabrication stage in filter design, another step is added during the power divided fabrication. Before printing the configuration on the tracing paper, the author needs to invert the image because the substrate used (Rogers Duroid 6006) is a negative photoresist material. In fact, a negative photoresist material indicated that the exposed region becomes hardened while the unexposed region will be removed in the fabrication stage. Hence, the net result of which the pattern formed is the reverse of the pattern in the tracing paper. In order to get the desired configuration, the inversion of the image is necessary. This problem will not happen in the filter fabrication stage because the filter designed is symmetrical. Inverting the configuration will not have any effect on the result.

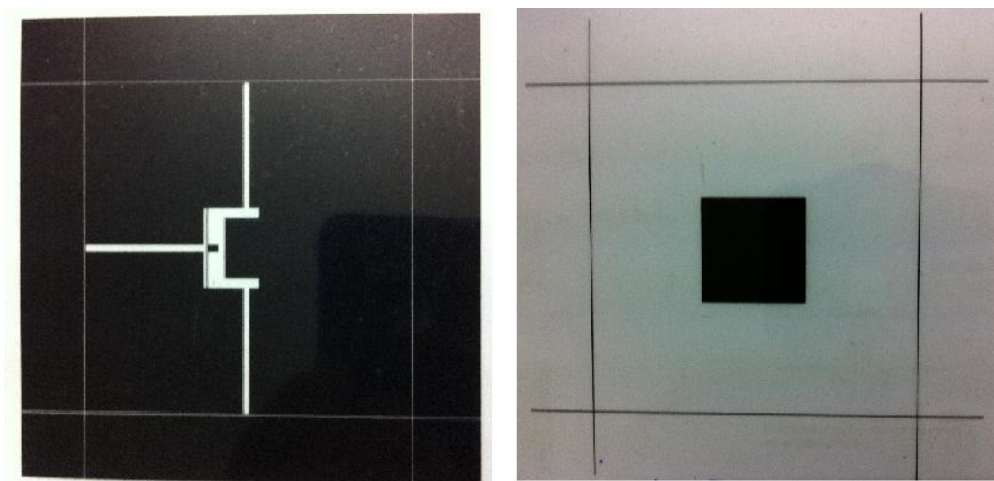


Figure 4.4: Printed tracing paper

### 4.2.3 Experiment Stage

Same machine, Rohde & Schwarz ZVB8 Vector Network Analyzer (VNA) is used to measure the experiment result. Calibration is needed to be completed before measuring the result. It aims to eliminate the effect of cable on measurement so that more accurate result can be obtained. As compare with the filter experiment, power divider experiment is more challenging and difficult in terms of that the author needs to look after one more output port. Equal values of transmission response ( $S_{21}$  and

$S_{31}$ ) are not easy to obtain, it is, however, necessary to be obtained because the author is designing a power divider of equalling output.

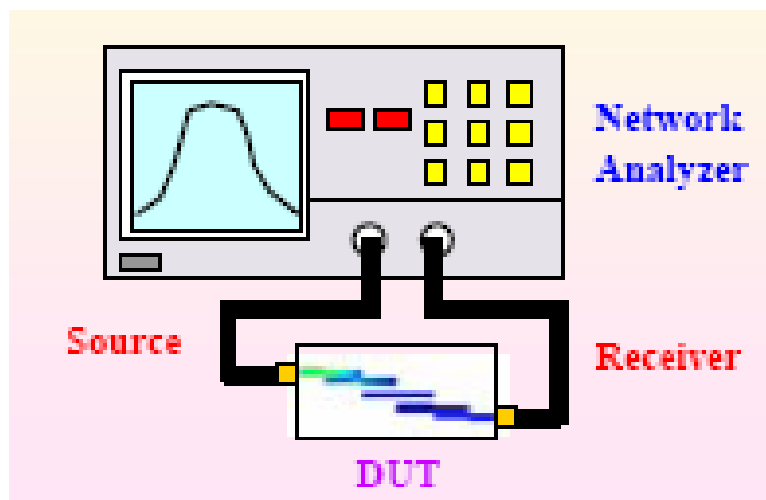


Figure 4.5: Experiment Stage

### 4.3 Proposed Filter Configuration

A dual-mode microstrip power divider has been designed successfully. The power divider designed is an electronic utility that is able to transmit input signal to two output ports equally. Same with the filter, the power divider designed has a cavity attached behind the substrate.

### 4.4 Results and Discussions

Figure 4.6 shows the comparison between the HFSS simulated and measured results. This figure shows the graphs of return loss or S-parameter ( $S_{11}$ ,  $S_{21}$  and  $S_{31}$ ). The measured result verified well the simulated results. Moreover, the different between the power divider phases ( $S_{21} - S_{31}$ ) is within 10dB. It means that the signal strength received by the two outputs is almost same. The desired microstrip power divider is designed.

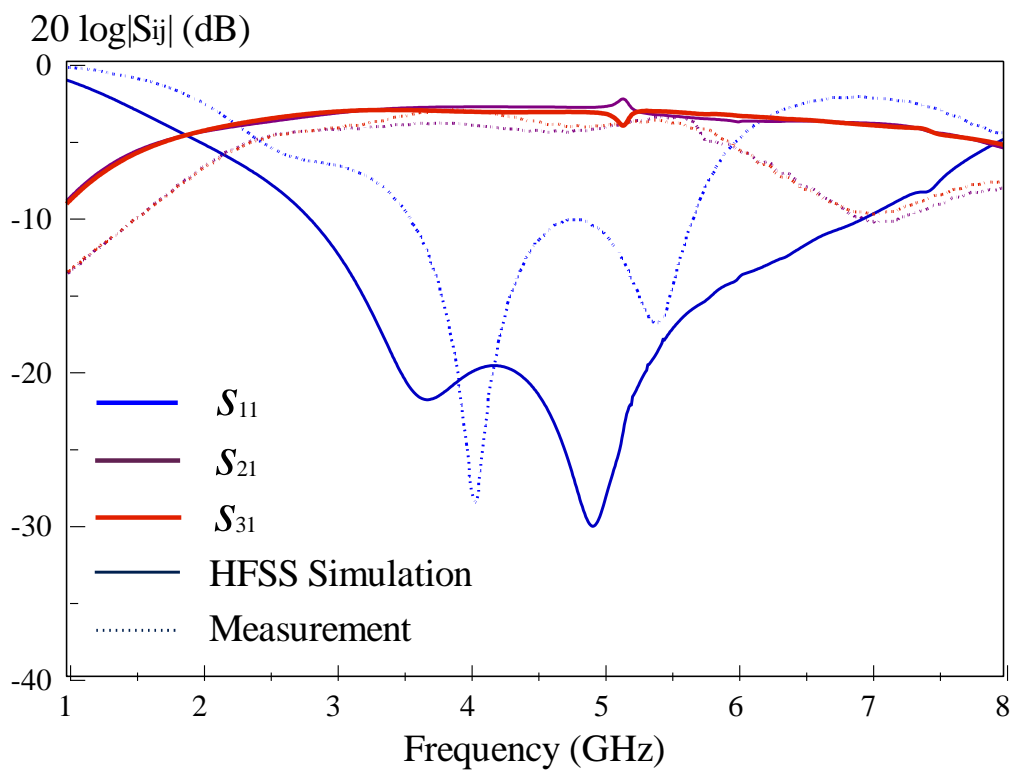


Figure 4.6: Comparison between simulated and measured result

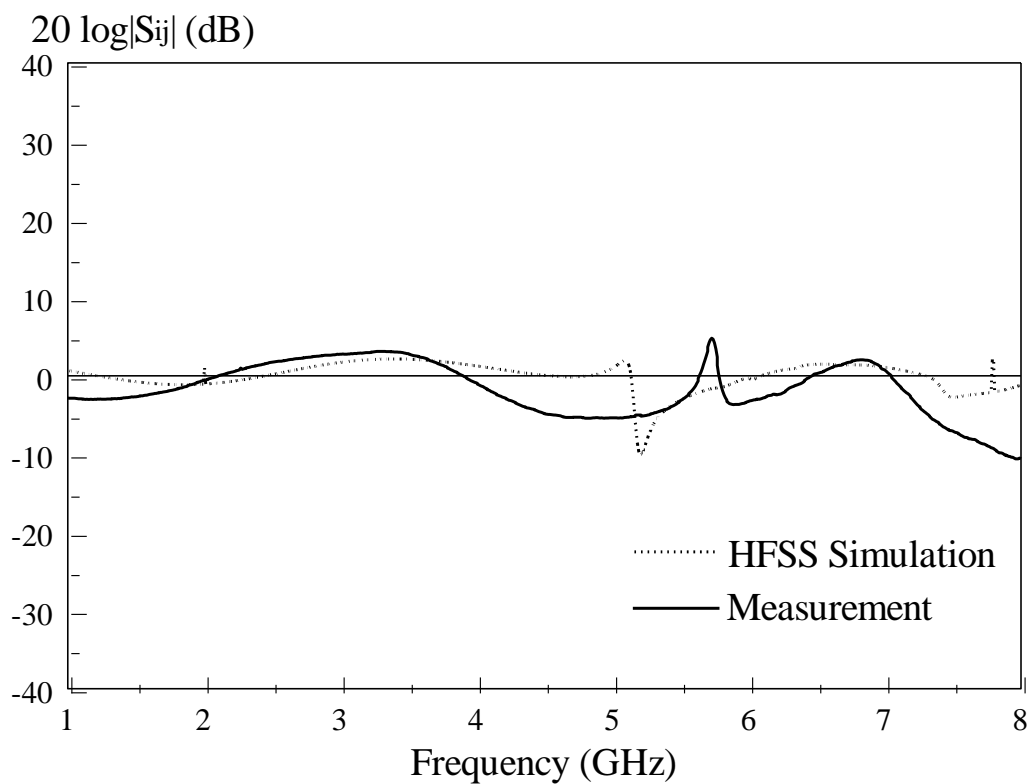


Figure 4.7: Difference between phases

By referring to Figure 4.6, the first order resonance, second order resonance and error between measured and simulated result can be calculated.

	Measured	HFSS	Error
First Resonance	4.06GHz	3.70 GHz	8.867%
Second Resonance	5.41GHz	4.93 GHz	8.872%

Besides, the central frequency,  $f_c$ , bandwidth and error between measured and simulated result can be calculated. The results are shown in the table below. The formulas used to calculate the center frequency, bandwidth and error are same as what been mentioned above.

	Measured		HFSS	
	$S_{21}$	$S_{31}$	$S_{21}$	$S_{31}$
Minimum Insertion Loss (dB)	-3.59	-3.14	-2.95	-3.15
3-dB Bandwidth (%)	-6.59	-6.14	-5.95	-6.15
$f_L$ (GHz) / $f_H$ (GHz)	2.07 / 6.27	2.17 / 6.12	1.489 / 8.131	1.481 / 8.499
$f_c$ (GHz)	4.170	4.145	4.810	4.990
Bandwidth (%)	100.719	95.296	138.087	140.641
Error (%)	0.000	0.000	13.306	16.934

#### 4.5 Case Studies

One of the power divider parameters will be manipulated during the case study. It aims to study the effect of parameters modification on the measured result and to find out if any modification of parameter will improve the power divider performance. For example, a lower power loss leads to wider passband and simpler configuration, and so on. The same frequency range with a simulated result is used

for an easier comparison purpose. Same with filter case study, two factors, which are distance of gap and dimension of cavity, are studied.

#### 4.5.1 Gap Distance

The author re-simulates the configuration after replacing the gap distance of power divider by 0.2mm and 0.3mm. By using 0.2mm and 0.3mm as gap distance, the two modes will be merged together and become a single mode. Moreover, the passband of power divider is narrower. It is definitely not an ideal case, hence, the gap value of 0.1mm is chosen eventually. As mentioned, 0.1mm is the minimum value that can be used for gap distance. If the gap distance used is lower than 0.1mm, it would be troublesome in the fabrication stage because it is hard to be printed on the tracing paper and fabricated on board.

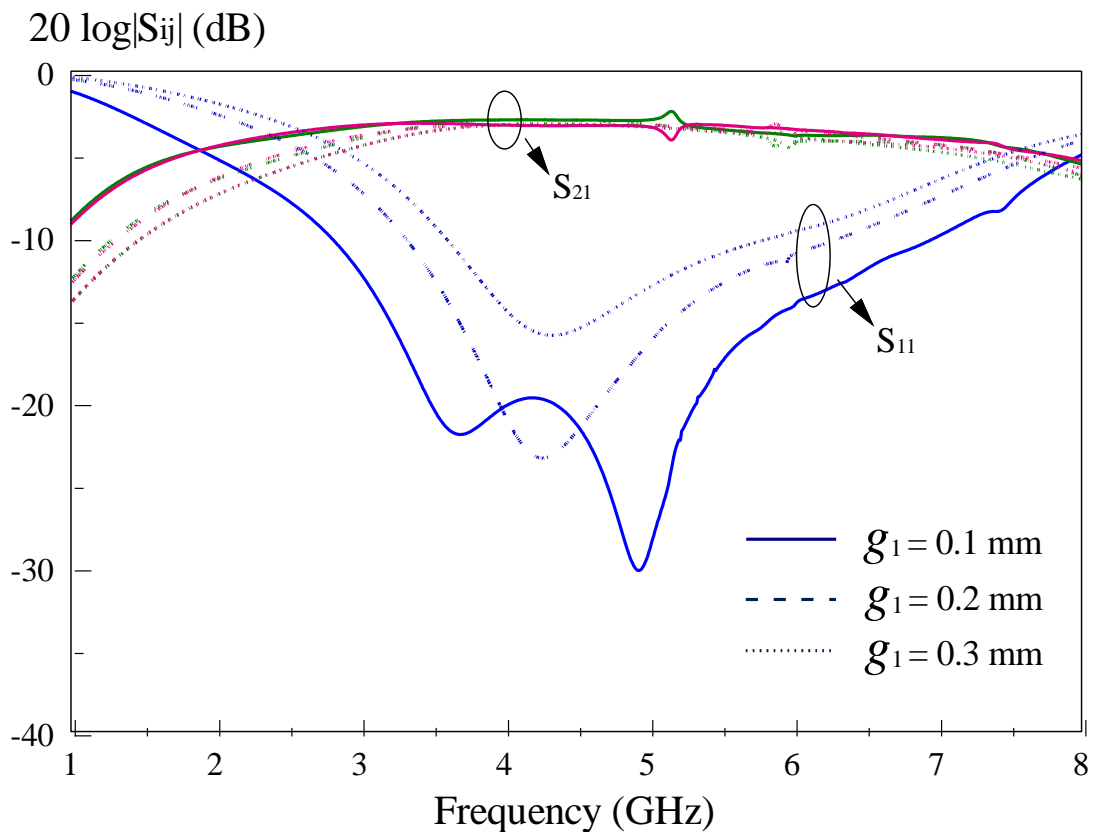


Figure 4.8: Effect of gap distance

## 4.5.2 Cavity Dimension

Different dimension of slots are studied. Dimension of slot can be divided into length, width and height. Manipulation of each of them would affect the result greatly.

### 4.5.2.1 Length of Cavity

The length of the cavity used in the present project is 16mm. From Figure 4.9, it can be seen that the two modes merged together whether the length of cavity is increased or decreased. This case is totally undesirable, so the value of 16mm is chosen.

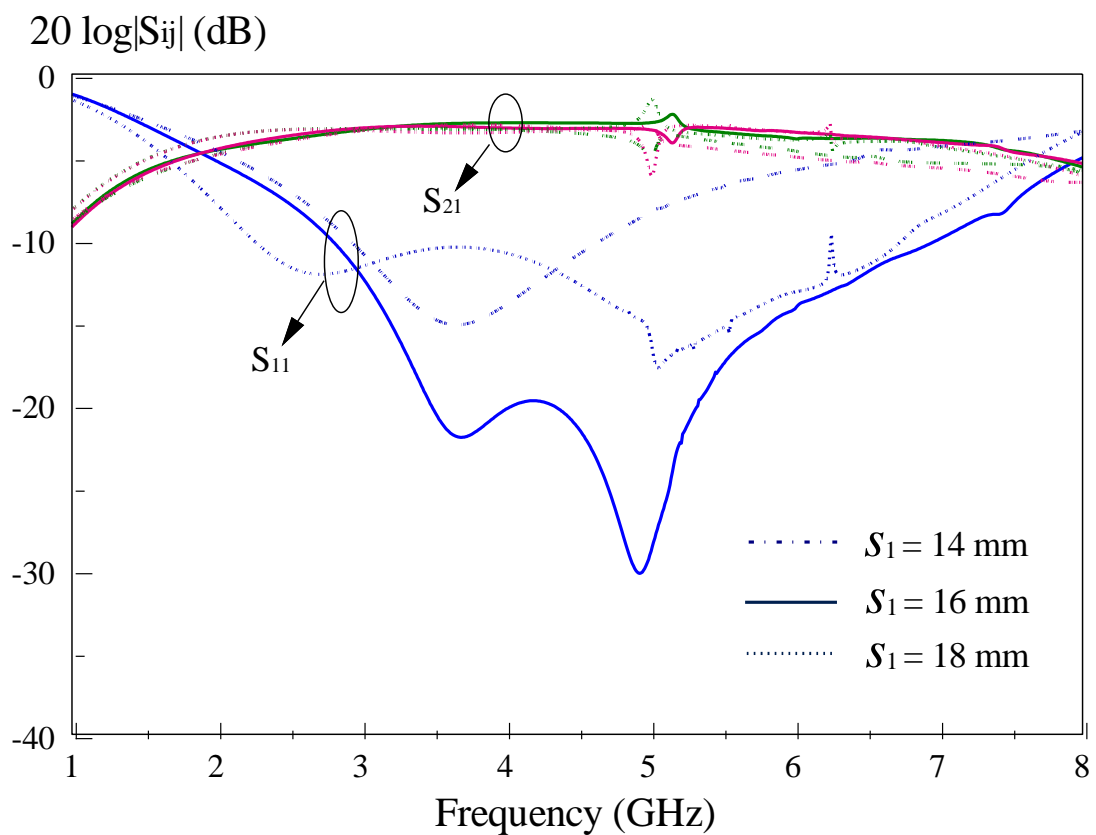


Figure 4.9: Effect of cavity length

#### 4.5.2.2 Width of Cavity

The same value which is of 16mm is used for the length and width of the cavity, but this does not mean that their case study will be same as seen from Figure 4.10. A different graph is obtained from the one shown in Figure 4.11. In this case, the simulated result is affected when the cavity width is changed to 14mm and 18mm. The centre frequency,  $f_c$  will be shifted into a lower or higher frequency.

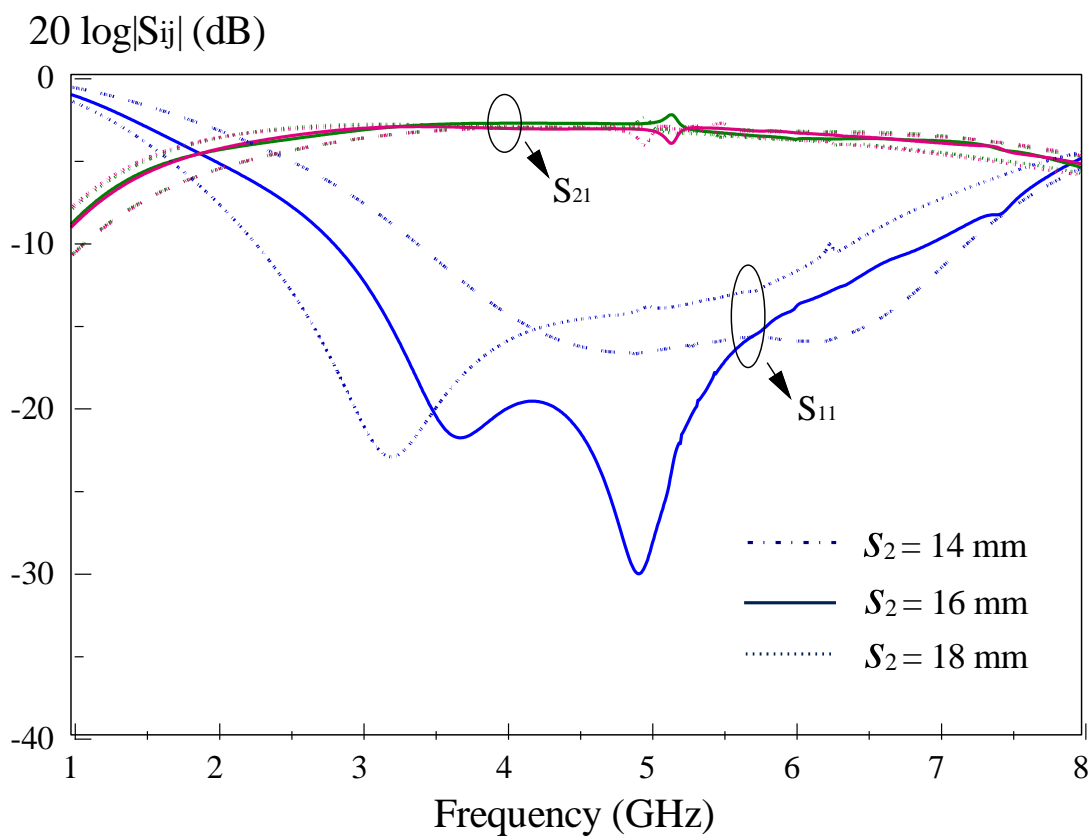


Figure 4.10: Effect of cavity width

### 4.5.2.3 Height of Cavity

The height of the cavity is also important. The cavity attached behind the board is the core idea in the power divider. In this case study, the author reduced the cavity height to 0mm in order to observe the effect of cavity. The result obtained is quite positive where it shows that the power divider is unable to function without the existence of the cavity. When the author increased the cavity height to 4mm, the  $S_{21}$  is affected. It indicated that not all the signals are transmitted from the input to the output ports. Some might be reflected due to the high  $S_{11}$  value. So, a 2mm of cavity height will get a better measured result and therefore it is selected.

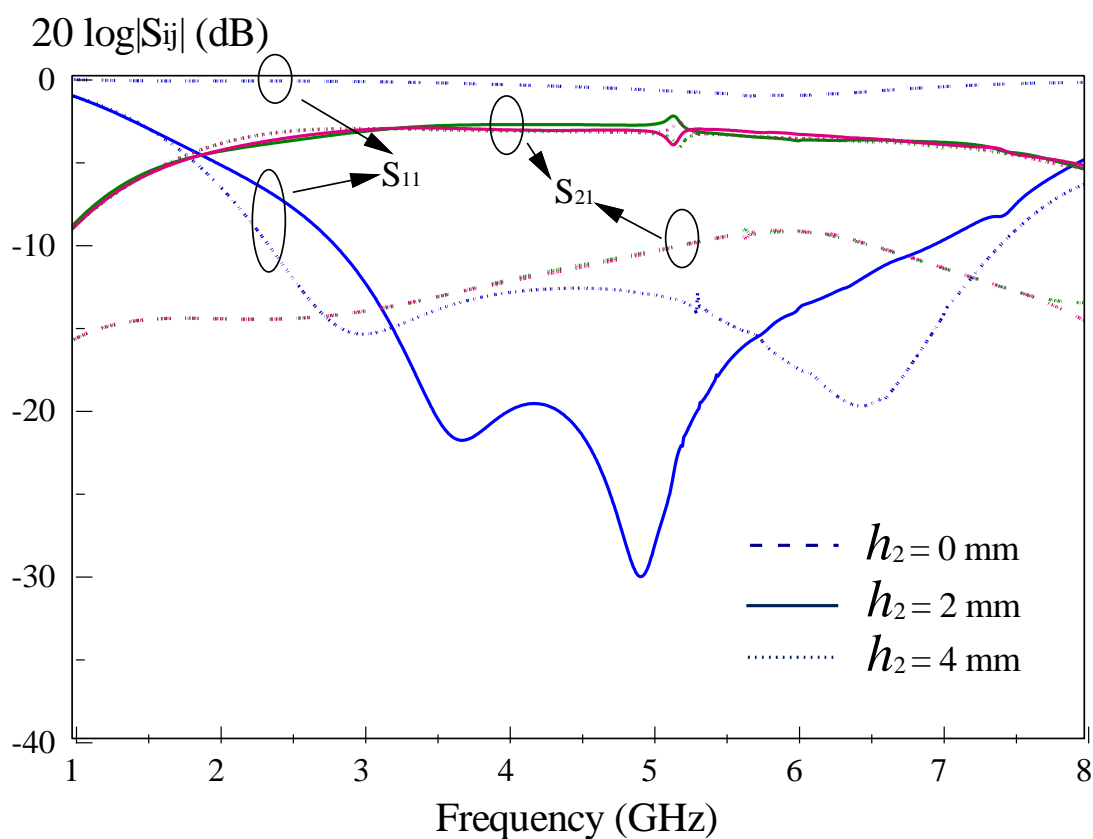


Figure 4.11: Effect of cavity height

## CHAPTER 5

### CONCLUSION AND RECOMMENDATIONS

#### 5.1 Conclusion

In this project, the idea of dual-mode microstrip bandpass filter and one-to-two microstrip power divider are proposed. Both of them have an attached cavity behind the board. With that attached cavity, the dual-mode property is showed in the filter and power divider successfully as proved in the case study. In fact, it is a creative idea in the IEEE journal since nobody had tried this type of project before. Ansoft HFSS simulation software was used to simulate the filter and power divider. The results agreed reasonably well with the measurement. It is hoped that the proposed idea would be useful for modern wireless systems.

In conclusion, a dual-mode microstrip bandpass filter and one-to-two microstrip power divider have been studied. Software and hardware are designed successfully. The reasonable agreement between the measured and simulated results is obtained. The objectives of this project have been achieved.

## 5.2 Recommendation

The microstrip power divider proposed has two outputs, where it can only be used in a specified purpose. It is unable to divide input signal into three outputs equally. So a one-to-three power divider is proposed. Its function is the same with the one-to-two power divider. The difference is only on the number of outputs. In fact, one is able to divide the input signal strength into three output ports equally. This will be very useful in the communication system since more outputs signal received equally. However, as what been mentioned, it will be more challenging as compared with the one-to-two power divider because the author needs to look after one more output port. It indicated that  $S_{41}$  will be added inside consideration. Moreover, equal strength of output signals should be received. It is not easy to get equal values of transmission response ( $S_{21}$ ,  $S_{31}$  and  $S_{41}$ ). Figure 5.1 shows the configuration proposed. Figure 5.2 is the simulated result obtained by simulating the proposed configuration. Figure 5.2 shows that  $S_{21}$ ,  $S_{31}$  and  $S_{41}$  have a same magnitude. It means that the strength of signal received in the three outputs is equal. Hence, it indicated that the proposed one-to-three power divider is working well and can be proceeded into the second stage, which is the fabrication stage. It will be a new study topic in power divider design in the future.

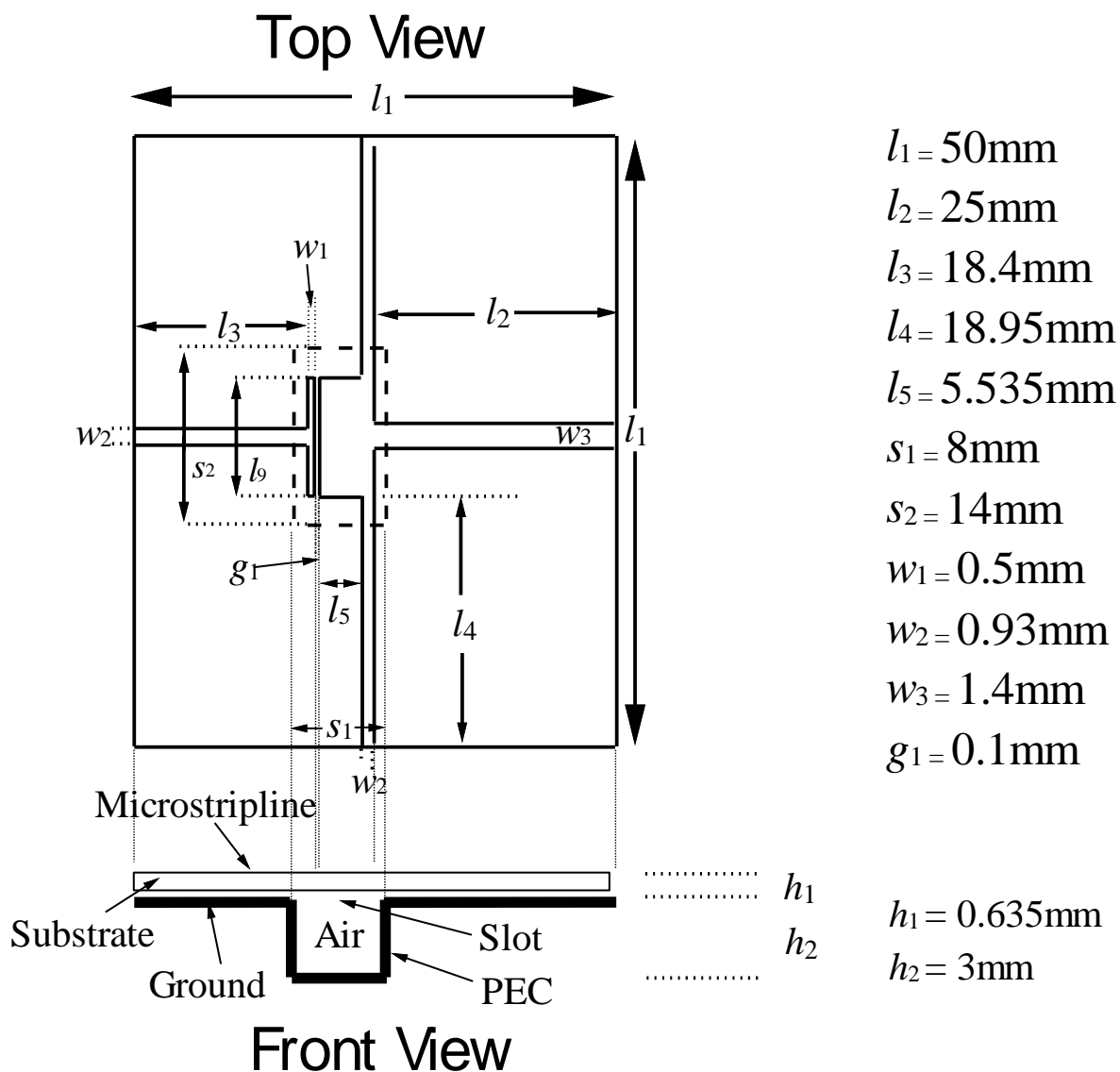


Figure 5.1: Proposed configuration of one-to-three microstrip power divider

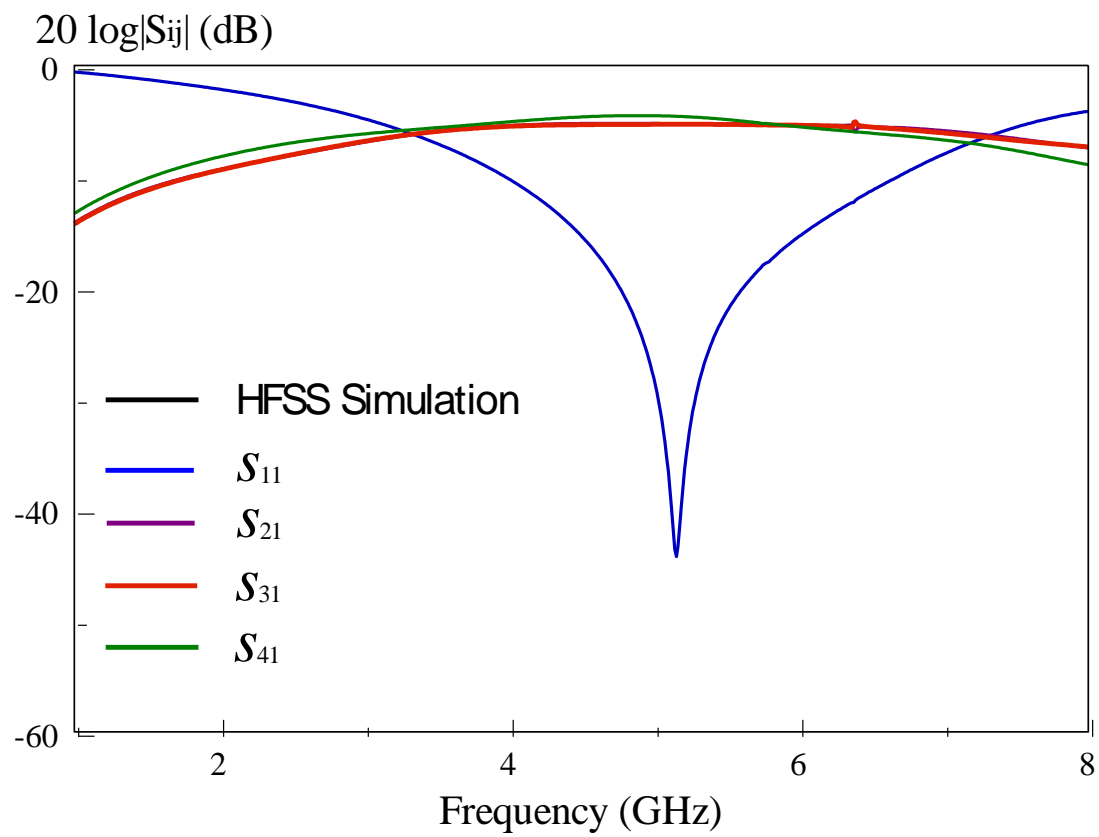


Figure 5.2: Simulated result

## REFERENCES

Hady, L.K, Kajfez, D, & Kishk, A.A. (2008, November 7). Dielectric Resonator Antenna in a Polarization Filtering Cavity for Dual Function Applications. *IEEE TRANSACTIONS ON MICROWAVE THEORY AND TECHNIQUES*, Volume: 56(Issue: 12).

Amari, S., & Rosenberg, U. (2005, October 31). Modular design of dual-mode filters using elliptic cavities. *Microwave Symposium Digest, 2005 IEEE MTT-S International* , 1255-1258.

Ahonnom, S., & Akkaraekthalin, P. (2009, December 10). Wideband Dual Mode Bandpass Filters with Wide Suppress Harmonics Using Notch Rectangular Slots and Interdigital Coupled Line. *Microwave Conference, 2009. APMC 2009. Asia Pacific* , 1439-1442.

Mitu, S.S.I., & Taiwo, S.L. (2010, July 11). Multilayer Unequal Microstrip Power Divider. *Antennas and Propagation Society International Symposium (APSURSI), 2010 IEEE* , 1-4.

Amari, S., & Seyfert, F. (2009, July 7). Design of Dual-Mode Ridge Cavity Filter. *Microwave Symposium Digest, 2009. MTT '09. IEEE MTT-S International* , 1625-1628.

Da-Peng Wang, Wen-Quan Che, & Russer, P. (2008, December 14). Tunable Substrate-Integrated Waveguide (SIW) Dual-Mode Square Cavity Filter with Metal

Cylinders. *Art of Miniaturizing RF and Microwave Passive Components*, 2008.  
*IMWS 2008. IEEE MTT-S International Microwave Workshop*

Lee, J.N., Yoo J.H., Kim J.H, Park J.K., Kim J.S., “The Design of UWB Bandpass Filter—Combined Ultra Wide Band Antenna”. Vehicular technology Conference pp 1-5, 2008

K. L. Wu, “An optimal circular –waveguide dual-mode filter without tuning screws”, *IEEE Trans. Microwave Theory Tech.*, vol. 47, pp. 271- 276, March 1999.

U. Rosenberg and S. Amari, “Novel design possibilities for dual-mode filters without intra-cavity couplings”, *IEEE Microwave Wireless Comp. Letters*, vol. 12, pp. 296-298, Aug. 2002.

L. Accatino, G. Bertin and M. Mongiardo, “Elliptical cavity resonators for dual-mode narrowband filters”, *IEEE Trans. Microwave Theory Tech.*, vol. 45, pp. 2393-2401, Dec. 1997.

Rui-Jie Mao, Xi ao-Hong Tang, "Novel Dual-Mode Bandpass Filters Using Hexagonal Loop Resonators", *IEEE Trans. On Microwave Theory and Techniques*-54 (2006), pp. 3526-3533